ELECTRONIC AND MICROWAVE PROPERTIES OF TRANSFERRED-ELECTRON SEMICOMDUCTORS(Dissertation_全文)

AUTHOR(S):

Sasaki, Akio

ELECTRONIC AND MICROWAVE PROPERTIES OF TRANSFERRED-ELECTRON SEMICONDUCTORS

BY

AKIO SASAKI

OCTOBER 1975

DEPARTMENT OF ELECTRONICS
KYOTO UNIVERSITY
KYOTO, JAPAN

ELECTRONIC AND MICROWAVE PROPERTIES OF TRANSFERRED-ELECTRON SEMICONDUCTORS

BY

AKIO SASAKI

OCTOBER 1975

DEPARTMENT OF ELECTRONICS
KYOTO UNIVERSITY
KYOTO, JAPAN

ABSTRACT

Electronic and microwave properties of transferred-electron semiconductors are investigated and described in this thesis. The thesis presents the following studies.

(1) The condition for differential negative resistance is obtained in transferred-electron semiconductors. With this condition, the confusion is resolved to the two operational modes: the mode based on the differential negative resistance and the mode based on the current instability.

(2) The conditions for space-charge-wave growth and differential negative resistance are derived with taking account of the energy transport effect. They can be considered to give more accurate quantitative results as compared with those derived precedently.

(3) The power-impedance product of the transit-time oscillation in transferred-electron diodes is obtained. The result predicts the maximum power output available from the transit-time oscillation. The formula for the maximum efficiency in the transit-time oscillation is also obtained.

(4) Self-pumped parametric effects in transferred-electron diodes are described. This study gives the theoretical basis to the self-pumped operation and the increase in the output power with a harmonic frequency.

(5) Transient behavior and characteristics of a high-field domain in transferred-electron diodes are analyzed with quasi-linear equations. In the analysis, the relaxation

time in a large-signal state, the equivalent admittance of a domain, the shape of a domain, the maximum value of a domain potential, and the current of a diode are described. The study gives a physical basis for non-linear and parametric operations of transferred-electron diodes.

(6) In the study on the magnetic field effects on the electron transfer and transport properties, it is found theoretically and experimentally that the magnetic field decreases not only the drift velocity along the applied electric field but also the energy in the random motion of the electrons in a single valley; the former is known as the magnetoresistance effect and the latter can be termed as the magnetic cooling effect. The cooling effect is interpreted due to the decrease in the drift velocity of electrons in each valley and the apparently reduced value of the collision time caused by the application of the magnetic field. A negative magnetoresistance effect is found in the velocity-field characteristic. The results obtained give the basis for the dynamic operations of transferred-electron diodes subjected to the crossed electric magnetic fields.

(7) Finally, in a further study on the electron properties of trnasferred-electron semiconductors, new wave instabilities caused by a negative dependency of the carrier temperature are derived. The analysis is equally valid for a collision-dominated, weakly ionized gas, although it is presented with reference to semiconductors.

ACKNOWLEDGMENTS

The author wishes to express his deep gratitude and appreciation to Professor Toshinori Takagi for his invaluable advice and encouraging, thoughtful guidance. The author wishes to thank Professor Tetsuro Tanaka for his stimulating discussions and criticism of the manuscript. The author is grateful to Professor Jun-ichi Ikenoue for his useful suggestions and criticism of the manuscript. The author acknowledges to Professors Yasuyuki Ohtani, Akira Kawabata, and Ryohei Itatani their stimulation to proceed with this study.

Appreciations are due to the late Professor Masazumi Terada of Osaka University for his comment on the differential susceptance and to Professor Hiroshi Hasegawa of Physics Department (Kyoto University) for his discussion on the wave instabilities. Appreciations are also due to Professors Masamitsu Nakajima and Hiroyuki Matsunami for constant discussions, and to Dr. Isao Yamada for his kind facilities on computer works.

The frequent discussions with Mr. Junji Saraie are appreciated. Thanks are due to Mr. Hidetoshi Oheda for his work in the experiment.

TABLE OF CONTENTS

TABLE OF CONTENTS, CONT'D

TABLE OF CONTENTS, CONT'D

LIST OF FIGURES

LIST OF TABLES

LIST OF PRINCIPAL SYMBOLS

SYMBOL

A	cross-sectional area of sample;
	term given in Eq. (8.16), in Chapter VIII
B	magnetic flux density (in z - direction);
	term given in Eq. (8.16), in Chapter VIII
C	geometrical capacity in Chapter II;
	bulk capacitance of diode in Chapter II;
	term given in Eq. (8.16), in Chapter VIII
C_d	capacitance of domain
C_d'	differential capacitance of diode
D	diffusion coefficient
D_e	diffusion coefficient
$D_{jj'}$	equivalent-intervalley deformation potential
D_{eff}	effective diffusion coefficient given by Eq. (8.23)
D_0	diffusion coefficient
D_1	diffusion coefficient in lower valley;
	field dependency of diffusion effect in Chapter VIII
D_2	diffusion coefficient in upper valley
D_{12}	intervalley deformation potential
E	applied electric field in Chapter VII;
	electric field in high-field domain
E_b	bias electric field
E_m	maximum electric field in high-field domain
E_s	sustaining electric field
E_0	dc electric field
E_v	valley electric field

LIST OF PRINCIPAL SYMBOLS, CONT'D

SYMBOL	
E_x	applied electric field (in x - direction)
E_y	Hall field (in y - direction)
E_1	microwave peak electric field
ΔE	domain excess electric field
ΔE_1	excess electric field in trailing edge of high-field domain
ΔE_r	excess electric field in leading edge of high-field domain
$\Delta E(0)$	initial amplitude of excess electric field
$\Delta E(x_0, t)$	maximum excess electric field
$E_0(t)$	electric field of high-field domain
G	bulk conductance of diode
I_0	direct current
I_1	amplitude of current with fundamental frequency in Chapter V; integration given by Eq. (7.11a)
I_2	amplitude of current with harmonic frequency in Chapter V; integration given by Eq. (7.11b)
I(t)	total current; current in diode in Chapter V
J	current density
J(t)	total current density
L	length of sample or diode
P_{abs}	absorbed power of sample

LIST OF PRINCIPAL SYMBOLS, CONT'D

SYMBOL	
S	stable region
$S(\omega)$	propagation constannt
T	electron or carrier temperature
T_0	lattice temperature
T_1	field dependency of carrier temperature
T_{L0}	lattice temperature
T_{L1}	field dependency of lattice temperature
T_{L00}	lattice temperature at zero external field
U	unstable region
V_b	bias voltage
ΔV	domain excess voltage
ΔV_c	rf voltage in circuit
$\Delta V(t)$	voltage of high-field domain
$\Delta V(0)$	initial amplitude of domain excess potential
$\Delta V_c(t)$	rf voltage in circuit
$\Delta V_0(t)$	high-field domain voltage due to only dc bias voltage
Z_r	resistive part of circuit impedance
a	normalization constant in Eq. (7.10)
e	absolute value of electron charge
f	frequency
f_1	symmetric term in distribution function of lower valley
f_2	symmetric term in distribution function of upper valley

LIST OF PRINCIPAL SYMBOLS, CONT'D

SYMBOL	
$f^{(1)}$	uniform and equilibrium function of Boltzmann's equation for lower valley
g_1	asymmetric term in distribution function of lower valley
g_2	asymmetric term in distribution function of upper valley
h	Planck's constant
$\hbar$	$h/2\pi$
k	length parameter by which value of excess electric field is assumed zero at cathode in Chapter VI; Boltzmann's constant in Chapter VIII; component of momentum
k	momentum vector
m_1	effective mass in lower valley
m_2	effective mass in upper valley
m*	effective mass
$m^{(N)}$	density-of-states mass
n	carrier density
n_T	total electron concentration
n_0	carrier density in Chapter II; doping concentration in Chapter VI; density of ionized impurity
n_1	electron concentration in lower valley
n_2	electron concentration in upper valley
q	electron charge

LIST OF PRINCIPAL SYMBOLS, CONT'D

SYMBOL	
r	concentration ratio
t	time
u	drift velocity of carriers in high-field domain
u_0	drift velocity of carriers in low-field region
$u_0(t)$	carrier drift velocity
v	drift velocity
v_d	total drift velocity; drift velocity of high-field domain in Chapter II
v_{ph}	phase velocity
v_{d1}	total drift velocity in lower valley
v_{d2}	total drift velocity in upper valley
v_0	drift velocity; average drift velocity in Chapter II
v_1	field dependency of carrier velocity in Chapter VIII
x'	coordinate moving with carrier drift velocity
x_{00}	position of disturbance occuring near cathode
Γ	propagation constant
Δ	high-field domain in prefix; term given by Eq. (8.20), not for prefix
α	field dependence of average drift velocity in Chapter II; parameter expressing diffusion effect and being zero when the effect is neglected, in Chapter III
β	phase constant; drift velocity taken account of diffusion and

LIST OF PRINCIPAL SYMBOLS, CONT'D

SYMBOL	
	energy transport effects, in Chapter III
γ	parameter expressing energy transport effect and being 1 when the effect is neglected, in Chapter III; energy ε when the band structure is parabolic, in Chapter VII
γ'	differentiation of γ with respect to energy ε and 1 when the band structure is parabolic, in Chapter VII
δ	ac component in prefix
ϵ	permittivity
ϵ_0	permittivity of free space
ε	dielectric constant; permittivity in Chapter VI; energy in Chapter VII
ε_0	energy difference between minimums of upper and lower valleys
ε_{t0}	total energy
ζ	term expressing differential mobility in Chapter III; coefficient to be determined by experiment in Chapter VII
θ	transit angle of carriers in sample; phase difference between fundamental and harmonic voltages in Chapter V
μ	mobility

LIST OF PRINCIPAL SYMBOLS, CONT'D

SYMBOL	
μ_L	mobility in low-field region
μ_d	mobility defined by $(u - u_0)/(E - E_0)$
$\bar{\mu}_d$	mobility μ_d averaged with respect to carrier density
ξ	coefficient to be determined by experiment
ρ	charge density in high-field domain
ρ_0	charge density of carrier; charge density of doping concentration in Chapter VI; low-field resistivity in Chapter VII
$\Delta\rho$	density of excess charge in high field domain, $\rho - \rho_0$
σ_0	average conductivity; low-field conductivity in Chapter VII
τ	collision time
τ_e	energy relaxation time
τ_T	thermal relaxation time
τ_{e0}	energy relaxation time
τ_{p0}	momentum relaxation time
ω	angular frequency
ω_c	inverse of dielectric relaxation time
ω_d	ratio of drift velocity squared to diffusion coefficient
ω_i	imaginary part of ω
ω_0	product of phase constant and dc velocity
ω_l	phonon angular frequency

LIST OF PRINCIPAL SYMBOLS, CONT'd

SYMBOL	
$\langle\ \rangle$	average in velocity space

SUPERSCRIPT SYMBOL	
(l)	lower valley
(N)	density of states
—	(not superscript symbol but bar) average with respect to lower and upper valleys in Chapter III

SUBSCRIPT SYMBOL	
b	bias
c	circuit
d	domain
1	fundamental frequency in Chapter V; lower valley in Chapter VII
2	harmonic frequency in Chapter V; upper valley in Chapter VII

CHAPTER I INTRODUCTION

In this thesis, electronic and microwave properties of transferred-electron semiconductors are studied.

To begin with, the study derives new small-signal instability due to the differential negative resistance in transferred-electron semiconductors being often called Gunn-effect semiconductors. The distinguishment is made between the instability of the differential negative resistance and the current instability. The maximum microwave power available from the current instability is predicted to the transit-time oscillation in transferred-electron diodes. A self-pumped operation of transferred-electron diodes is analyzed with taking account of an rf circuit voltage.

The transient behavior and large-signal characteristics of the current instability are analyzed using qausi-linear equations. The analysis derives the equivalent impedance of transferred-electron diodes in transient and stable states. With this equivalent impedance, the self-pumped operation of transferred-electron diodes is interpreted.

The magnetic field effects on transferred-electron characteristics are studied deriving the electron distribution functions. It is found and described that the raise in the carrier temperature is suppressed by the application of a magnetic field. It can be termed the magnetic cooling effect. The negative magnetoresistance effect is found in the region of a negative differential mobility. This effect is understood as the result from

the magnetic cooling effect. These are confirmed qualitatively in experiments. The velocity-field characteristic derived in this study gives the basis on the study of the dynamic characteristics of transferred-electron diodes subjected to the crossed electric and magnetic fields.

Finally, the study extends to the wave instabilities based on the field-dependent drift velocity and carrier temperature. It predicts new wave instabilities due to the negative dependency of the temperature variations on the electric field and compare with previous diffusion instability.

Through these subjects, the thesis describes electronic and microwave properties of transferred-electron semiconductors.

The transferred-electron effect semiconductors are a synonym in other expressions for the transferred-electron semiconductors. The latter is used throughout the thesis for simplicity.

CHAPTER II CONDITIONS FOR AMPLIFICATION AND OSCILLATION IN TRANSFERRED-ELECTRON SEMICONDUCTORS

Experiments have shown that there are two operational modes in bulk GaAs:[1] one is the mode which is less dependent on the external load and can be used only as an oscillator,[2] and occurs in a low-resistivity sample; the other is the mode which is much more dependent on the external load can be used as either amplifier[3], [4] or oscillator,[1] and occurs in a high-resistivity sample. From the equivalent impedance of a GaAs bulk semiconductor, we will examine the difference between two modes and find the condition for the second mode to occur.

We may consider that the first mode is due to the current instability analyzed by McCumber and Chynoweth.[5] The current instability can occur when the differential negative conductance of a sample is infinite and the susceptance changes from the capacitive to inductive near the critical condition. The oscillation due to the current instability may start nearly independent of the external load. We can consider that the second mode is taken to occur when a sample is operated in a region where finite negative conductance and finite susceptance are realized at a bias voltage below that for the current instability to occur. Hence, the second mode is used as oscillator or amplifier depending on whether the negative conductance exceeds the load conductance.

A small-signal analysis may be used to derive the equivalent impedance of a GaAs bulk semiconductor:[6]

$$Z_e = \frac{(\alpha\omega_c/\omega) - j}{\omega C\{1 + (\alpha\omega_c/\omega)^2\}} \cdot \frac{1 + \Gamma L - e^{\Gamma L}}{\Gamma L}, \tag{2.1}$$

where the propagation constant Γ is

$$\Gamma = \frac{\omega_d}{2v_0}\left\{1 - \sqrt{1 + 4\frac{\alpha\omega_c}{\omega_d} + 4j\frac{\omega}{\omega_d}}\right\}. \tag{2.2}$$

Here $\alpha = E_0(d \ln v_0/dE_0)$ is the field dependence of average drift velocity v_0 in the conduction band of GaAs, $\omega_c = \sigma_0/\epsilon$ is the ratio of the average conductivity σ_0 to the permittivity ϵ, $\omega_d = v_0^2/D_e$ is the ratio of a drift velocity squared to the diffusion coefficient D_e determined by the Einstein relation $D_e = \mu kT/e$, and $C = \epsilon A/L$ is the geometrical capacity where A and L are the cross-sectional area and the length of a sample, respectively. We analyze the case when $(\omega/\omega_d)^2 \ll 1$ is satisfied.

As McCumber and Chynoweth reported, a first zero of the impedance occurs at $\alpha\omega_c/\omega = -0.280$ and $\omega L/v_0 = 2.38\pi$, which give the critical condition for the current instability. From both conditions they obtained the condition for the current instability in a GaAs bulk semiconductor:[5]

$$n_0 L > 2.7 \times 10^{11}\ \mathrm{cm}^{-2} \tag{2.3}$$

where n_0 is the carrier density. We may point out that in a sample the oscillation starts at $\omega = 2.38\pi v_0/L$ and then, when stable oscillation is achieved, the frequency is given by $\omega = 2\pi v_d/L$ where v_d is the drift velocity of the high-field domain.

We find next the critical condition at which negative

resistance occurs in a GaAs bulk semiconductor. We consider that it can occur with small value of $\alpha\omega_c/\omega_d$. Then the equivalent resistance, the real part of Eq. (2.1), can be reduced to

$$R_e \cong \frac{1}{\omega C\theta_e}\left[1+\frac{\alpha\omega_c}{\omega}\theta_e-\left\{1-\left(\frac{\alpha\omega_c}{\omega}+\frac{\omega}{\omega_d}\right)\theta_e\right\}\cos\theta_e\right] \qquad (2.4)$$

where $\theta_e=\omega L/v_0$ is the transit angle of carriers in a sample. A first negative value occurs at $\omega L/v_0=2\pi$ (except for $\omega L/v_0=0$). The condition for the resistance to be negative is $(-\alpha)\omega_c/\omega>\omega/2\omega_d$. This indicates that the semiconductor exhibits a negative resistance when the value of the conduction current of a forward space-charge wave in a GaAs semiconductor exceeds a half value of the diffusion current, since $(-\alpha)\omega_c/\omega$ expresses the ratio of the conduction current to the displacement current and ω/ω_d expresses the ratio of the diffusion current to the displacement current. The condition is written as

$$n_0L^2 > \frac{2\pi^2\epsilon(kT/e)}{e(-\alpha)} \qquad (2.5)$$

where e is the absolute value of electron charge,

$$kT/e = k\{T_0 + (2/3)\tau_T v_0 E_0\}/e$$

is the electron temperature, T_0 is the lattice temperature, and τ_T is the thermal relaxation time. From the condition at which a GaAs bulk semiconductor exhibits a maximum negative value of $E_0(d\ln v_0/dE_0)$ derived by McCumber and Chynoweth,[5] we know the numerical values: $\alpha=-0.272$ and $kT/e\cong 0.092$ volt. Using the values $\tau_T=2\times10^{-12}$ sec and $\epsilon=12.5\epsilon_0$ (ϵ_0 is the permittivity of free space),

we obtain

$$n_0 L^2 > 4.6 \times 10^7 \text{ cm}^{-1} \qquad (2.6)\ [7]$$

which is in a good agreement with the condition of minimum nL^2 product calculated from the experimental values n and L listed in reference [1].

We can show that the condition for the resistance of the semiconductor to be negative is different from the condition for the forward space-charge wave to grow. The condition for the real part of Eq. (2.2) to be positive is $(-\alpha)\omega_c/\omega > \omega/\omega_d$, which is rewritten as

$$\frac{n_0}{f^2} > \frac{4\pi^2\epsilon(kT/e)}{e(-\alpha)v_0^2} = 9.2 \times 10^{-7} \text{ (c/s)}^{-2} \text{ cm}^{-3}, \qquad (2.7)$$

where we used the numerical values of T, $(-\alpha)$, and v_0 given by McCumber and Chynoweth.[5] The condition $(-\alpha)\omega_c/\omega > \omega/\omega_d$ is also obtained from that for the resistance associated with forward space-charge wave to be negative.

At the condition for the current instability, we know from $\alpha\omega_c/\omega = \alpha\sigma_0/\epsilon\omega = -0.280$ that a low-resistivity sample requires a smaller value of α than a high-resistivity sample. The low-resistivity sample ($n_0 L \gg 2.7\times10^{11}$ cm^{-2}) as used in Gunn's experiment[2] can satisfy the instability condition slightly beyond the threshold bias voltage. If a high-resistivity sample satisfies the condition, $n_0 L^2 > 4.6\times10^7$ cm^{-1}, $n_0 L < 2.7\times10^{11}$ cm^{-2}, then only a finite admittance occurs in the sample. Thus, the operational conditions, amplification or oscillation, of a high-resistivity sample depend on the external load. If a sample has a value

slightly larger than $n_0L = 2.7\times10^{11}\ \mathrm{cm}^{-2}$, then the two operational modes, the current instability and the other, are realizable in the same sample depending on the bias voltage.

CHAPTER III CONDITIONS FOR SPACE-CHARGE-WAVE GROWTH AND DIFFERENTIAL NEGATIVE RESISTANCE IN TRANSFERRED-ELECTRON SEMICONDUCTORS

McCumber and Chynoweth[1] have derived the impedance of a bulk semiconductor in which the carrier velocity depends non-linearly on the electric field as a result of the two valleys in the conduction band. They have obtained the condition for zero impedance which permits current instability to occur in a bulk semiconductor. We may consider two other conditions: one is the condition for a space-charge wave to grow in a bulk semiconductor; the other is the condition for the differential negative resistance which permits oscillation when the differential negative conductance of the bulk semiconductor exceeds the load conductance. These conditions are not simply given by the differential negative mobility when we taken into account the diffusion effect which prevents the space-charge wave from growing and the resistance from being negative. To see the conditions for amplification and oscillation in the bulk semiconductor, both conditions have been obtained from the small-signal wave theory[2] in which the diffusion effect was considered only in terms of $\bar{\mu}T(\partial n/\partial x)$ and the electron temperature was approximated by $T \cong T_0 + (2\tau_T \bar{\mu} E^2/3)$. In this chapter, two conditions will be derived from the impedance given by McCumber and Chynoweth in which both diffusion and energy-transport effects are taken into account. With the condition for the differential negative resistance, the work described here will thus add one condition for the small-signal instabilities.

The condition for space-charge-wave growth requires that the real part of the propagation constants $s(\omega)$ given by McCumber and Chynoweth's equation (41b) must be positive. Noting that $\exp(-i\omega)$ was used in (41b) and considering the first-order approximation for the diffusion effect α to be small, we obtain $-\bar{\zeta}/\gamma\omega > \alpha\gamma\omega/\beta$ which indicates that the effect of a differential negative mobility $\bar{\zeta}$ must be larger than the effect of the diffusion α. The condition can be written as

$$\frac{n_0}{f^2} > \frac{4\pi^2\epsilon T}{e\left(-E\dfrac{d}{dE}\ln\bar{v}\right)\bar{v}^2}\left(1+\frac{E}{2}\frac{d\ln\bar{\mu}}{dE}\right)\left(\frac{\gamma\bar{v}}{\beta}\right)^2 \tag{3.1}$$

where $\gamma \neq 1$ when the energy transport is considered and $\beta \neq \bar{v}$ when both diffusion and energy transport are considered,[1] and we follow the notations used by McCumber and Chynoweth except that ϵ is the permittivity of the semiconductor. From the negative condition on the real part of the impedance $Z(\omega)$ given in (41a), we obtain $-\bar{\zeta}\gamma\omega > \alpha\gamma\omega/2\beta$ at $\gamma\omega L/\beta = 2\pi$. It can be written as

$$n_0 L^2 > \frac{2\pi^2\epsilon T}{e\left(-E\dfrac{d}{dE}\ln\bar{v}\right)}\left(1+\frac{E}{2}\frac{d\ln\bar{\mu}}{dE}\right) \tag{3.2}$$

which can be considered to be the condition for one of the small-signal instabilities. We may expect the small-signal instability by which the space-charge-wave growth breaks into the oscillation[3] only when the differential negative conduct-

ance exceeds the load conductance. Otherwise the amplification which has been experimentally shown by Thim et al. may be expected.[4] We see that there are additional terms, $(E/2)(d \ln \bar{\mu}/dE)$ and $(\gamma\bar{v}/\beta)^2$, in the conditions given here as compared with the conditions derived from the small-signal wave theory.[2] The discrepancy results from the difference in the assumptions of the two analyses.

In a GaAs bulk semiconductor, for example, a minimum value of the derivative $d \ln \bar{v}/dE$ is -5.43×10^{-3} m/V at $E = 5 \times 10^5$ V/m where the value[5] of the average velocity $\bar{v}$ is 1.00×10^5 m/s. Using the value of the thermal relaxation time $\tau_T = 2 \times 10^{-12}$ second, the permittivity $\epsilon = 12.5\epsilon_0$ and the lattice temperature $T_0 = 0.025$ eV,[1] we obtain

$$n_0/f^2 > 3.4 \times 10^{-7}(\gamma\bar{v}/\beta)^2 \text{ cm}^{-3}(\text{c/s})^{-2} \tag{3.3}$$

and

$$n_0 L^2 > 1.7 \times 10^7 \text{ cm}^{-1}. \tag{3.4}$$

CHAPTER IV FREQUENCY DEPENDENCIES OF POWER AND EFFICIENCY OF TRANSIT-TIME OSCILLATIONS IN TRANSFFERRED-ELECTRON SEMICONDUCTORS

When the voltage V_b is applied to a sample of a bulk semiconductor which is uniformly doped along a length L, a uniform electric field E_b is applied to the sample:

$$V_b = E_b L. \tag{4.1}$$

As discovered by Gunn,[1] a disturbance in the field at the cathode contact (low-voltage side) of a sample grows to a high-field domain when the field E_b is in the range, beyond the threshold and below the valley field E_v, where bulk semiconductors such as GaAs and InP show a negative differential mobility. The high-field domain drifts from the cathode contact to the anode contact (high-voltage side) of the sample and is extinguished at the anode. The repetition of growth, drift, and extinction induces an rf voltage ΔV_c in the circuit. The rf circuit voltage reduces the bias voltage of the sample to the value $(V_b - \Delta V_c)$ when the phase of the rf circuit voltage is opposite to the polarity of the applied dc voltage V_b. The high-field domain is quenched when the rf voltage ΔV_c reduces the field in the sample to below the sustaining field E_s, which is the minimum strength of the field necessary to sustain the transit-time oscillation. In order to sustain the transit-time oscillation in the sample, we require

$$E_b L - \Delta V_c > E_s L. \tag{4.2}$$

From Eq. (4.2), the rf power P delivered to the circuit is

given by

$$P < \frac{(E_b - E_s)^2 v_d^2}{2f^2 Z_r}, \tag{4.3}$$

where Z_r is the resistive part of the impedance of the circuit, f is the oscillation frequency, v_d is the average drift velocity of the high-field domain, and the equation $f \cong v_d/L$ is used since the frequency of the transit-time oscillation is determined by the transit time of the high-field domain. The power-impedance product (PZ_r) of the transit-time oscillation in a transferred-electron semiconductor is proportional to the square of the product of the difference of the applied and the sustaining fields and the drift velocity, and inversely proportional to the square of the frequency. It is very interesting to notice that Eq. (4.3) shows a result similar to that of the physical limitation on power of transistors given by Johnson.[2] The dc power supplied to a sample is given by $P_d = ALE_b \cdot \langle J(t) \rangle$, where A is the cross-sectional area of a sample and $\langle J(t) \rangle$ is the average current density in the transit-time oscillation. The efficiency $\eta = P/P_d$ is obtained by

$$\eta < \left(1 - \frac{E_s}{E_b}\right)^2 \frac{v_d E_b}{2Af Z_r \cdot \langle J(t) \rangle}, \tag{4.4}$$

which indicates that the efficiency-impedance product (ηZ_r) of the transit-time oscillation is inversely proportional to the frequency. In the case of the quenched mode, the value of the field strength in the right-hand side of Eq. (4.2)would be less than the value of the E_s and the length in the equation $f \cong v_d/L$ would be a fraction of the length L, but the results of Eqs. (4.3)

and (4.4) are not much modified. The results, however, are changed when there is impact ionization in the high-field domain.

The value of the power-impedance product (PZ_r) of the transit-time oscillation in uniformly-doped n-GaAs, for example, is

$$PZ_r < \frac{28800}{f^2} \qquad (4.5)$$

in watts·GHz. It was assumed that the average drift velocity $v_d \cong 10^5$ m/s and the sustaining field $E_s \cong 10^5$ V/m, and that the sample is biased near the valley field $E_v = 25 \times 10^5$ V/m.[3]

CHAPTER V SELF-PUMPED PARAMETRIC AMPLIFICATION AND OSCILLATION OF TRANSFERRED-ELECTRON SEMICONDUCTORS

It is by now well known that in a transferred-electron diode oscillating in a transit-time mode a high-field domain grows near the cathode and travels in a stable state through the diode and is quenched at the anode. A high-field domain consisting of charge-accumulation and charge-depletion regions can be represented by a capacitance.[1] The capacitance is observed in a diode during the transit of a high-field domain, and disappears with extinction of a high-field domain at the anode. The admittance of the domain varies with time during the transient periods near the cathode and at the anode.[2] Thus the repetition of growth, transit, and extinction of the domain leads to the repeated change in a admittance of the transferred-electron diode. The admittance change is repeated with the frequency of an oscillating diode. The self-pumped parametric amplification and oscillation of the transferred-electron diodes were previously treated by considering the appearance and the disappearance of the domain capacitance[1], [3]-[5] and the change of the domain admittance in transient periods.[2], [6], [7]

The effect of an external rf voltage on the admittance of a stable domain was not taken into account in previous treatments. For reference the dependence of the domain capacitance on the bias voltage is shown in Fig. 5.1 where the capacitance has been calculated using the results of the large-signal theory.[2] In this chapter the self-pumped parametric effect is presented where the bias voltage across a diode is varied by

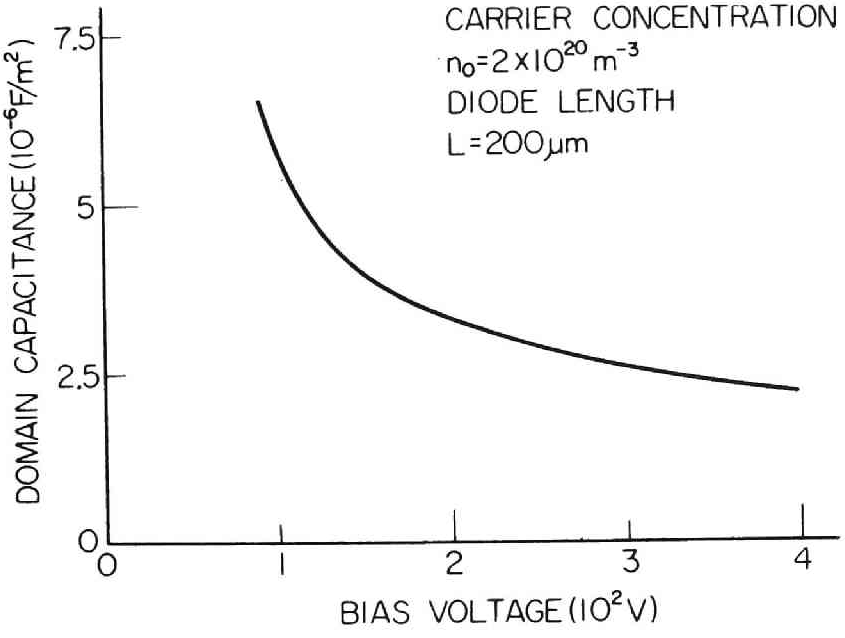

Fig. 5.1 Dependence of domain capacitance on bias voltage.

the rf output voltage. There can be considered two cases in self-pumped parametric operations: one is the external-signal amplification by the parametric change of the admittance of a diode self-pumped by the voltage with a fundamental frequency of the oscillating diode; the other is the oscillation increased in the output power by the additional negative conductance of a diode self-pumped by the voltage with a harmonic frequency of the oscillating diode.

We consider a transferred-electron diode of length L and biased with dc voltage V_b. When the bias field exceeds the threshold field, a high-field domain of voltage $\Delta V(t)$ grows in a diode. Thus current flows in an rf circuit, and an rf voltage is induced across the rf circuit. The dc bias voltage is

changed by the superposition of this rf voltage. The total bias voltage must be equal to the total voltage obtained from the field distribution inside the diode.

$$V_b + \Delta V_c(t) = E_0(t)L + \Delta V(t) \tag{5.1}$$

where $\Delta V_c(t)$ is the rf voltage, and $E_0(t)$ is the electric field outside the domain (i.e., in the low-field region) and is assumed uniform in space. The current $I(t)$ in a diode can be given in terms of the conditions outside the domain

$$I(t) = A\rho_0 u_0(t) + A\varepsilon \frac{\partial}{\partial t} E_0(t) \tag{5.2}$$

where the first term represents the conduction current and the second the displacement current. Here A denotes the constant cross-sectional area of the diode, ρ_0 the charge density of carriers, $u_0(t)$ the carrier drift velocity given by $\mu E_0(t)$, and ε the dielectric constant. The substitution of $E_0(t)$ from Eq. (5.1) into Eq. (5.2) gives

$$I(t) = GV_b + G\{\Delta V_c(t) - \Delta V(t)\} + \frac{\partial}{\partial t}[C\{\Delta V_c(t) - \Delta V(t)\}] \tag{5.3}$$

where $G = A\rho_0\mu/L$ represents the bulk conductance of a diode at the low field and $C = A\varepsilon/L$ the bulk capacitance of the diode.

We consider first the parametric change in admittance of a diode self-pumped by the voltage with a fundamental frequency. The rf voltage across a diode is then expressed as $\Delta V_c(t) = \Delta V_{c1} \sin \omega t$, which is superposed on the dc voltage V_b. The domain voltage $\Delta V(t)$ depends non-linearly on the bias voltage.[2] In order to see the effect of the rf voltage $\Delta V_c(t)$ on the domain

voltage $\Delta V(t)$, we expand the domain voltage in terms of the rf voltage.

$$\Delta V(t) = \Delta V_0 + \alpha \Delta V_{c1} \sin \omega t + \beta (\Delta V_{c1} \sin \omega t)^2 + \cdots \tag{5.4}$$

where

$$\alpha = \left[\frac{\partial \Delta V}{\partial \Delta V_c}\right]_{\Delta V_c = 0} \quad \text{and} \quad \beta = \frac{1}{2}\left[\frac{\partial^2 \Delta V}{\partial \Delta V_c^2}\right]_{\Delta V_c = 0}$$

Here ΔV_0 represents the domain voltage which is due to only the dc bias voltage, and is constant in the stable state. Substituting Eq. (5.4) into (5.3), we obtain

$$I(t) = GV_b - G\Delta V_0 + G(1 - \alpha - \beta \Delta V_{c1} \sin \omega t \cdots)\Delta V_{c1} \sin \omega t + \frac{\partial}{\partial t}\{C(1 - \alpha - \beta \Delta V_{c1} \sin \omega t \cdots)\Delta V_{c1} \sin \omega t\} \tag{5.5}$$

which describes the relationship between the current $I(t)$ and the rf voltage $\Delta V_c(t)$. We can see in Eq. (5.5) that there is a parametric change in conductance and capacitance, given by $G\beta\Delta V_{c1}$ and $C\beta\Delta V_{c1}$, with the frequency $\omega/2\pi$. Using this self-pumped parametric change in admittance, we can obtain the amplification of a signal supplied from an external source to an oscillating diode.

We present next the admittance of a diode self-pumped by a voltage of the second harmonic. The rf voltage across a diode is then

$$\Delta V_c(t) = \Delta V_{c1} \sin \omega t + \Delta V_{c2} \sin (2\omega t + \theta) \tag{5.6}$$

where θ is the phase difference between the fundamental and the harmonic voltages. The current $I(t)$ can be written as

$$I(t) = I_0 + I_1 \sin(\omega t + \psi_1) + I_2 \sin(2\omega t + \psi_2) \tag{5.7}$$

where I_0 denotes the direct current, I_1 and I_2 the amplitudes of the current with fundamental and harmonic frequencies, respectively, and Ψ_1 and Ψ_2 the phase difference with respect to the voltage $\Delta V_{c1} \sin \omega t$. The domain voltage is, as before, expanded in terms of the rf voltage $\Delta V_c(t)$ as

$$\Delta V(t) = \Delta V_0 + \alpha \Delta V_c(t) + \beta \Delta V_c(t)^2 + \cdots. \tag{5.8}$$

Substituting Eqs. (5.7) and (5.8) into Eq. (5.3) and taking the terms of the fundamental frequency, we obtain

$$I_1 \sin(\omega t + \psi_1) = \bar{G}_d \Delta V_{c1} \sin \omega t + \omega \bar{C}_d \Delta V_{c1} \cos \omega t \tag{5.9}$$

where

$$\begin{aligned} \bar{G}_d &= G\left\{1 - \alpha + \beta \Delta V_{c2}\left(\sin\theta + \frac{\omega C}{G}\cos\theta\right)\right\} \\ \bar{C}_d &= C\left\{1 - \alpha + \beta \Delta V_{c2}\left(\sin\theta - \frac{G}{\omega C}\cos\theta\right)\right\}. \end{aligned} \tag{5.10}$$

Here $\bar{G}_d$ and $\bar{C}_d$ are the conductance and the capacitance, respectively, of a diode self-pumped by a voltage of the second harmonic. We can see in Eq. (5.10) an additional conductance that can be negative by properly choosing the phase of the second harmonic with respect to the fundamental wave. We can thus obtain an increase of output power of a diode self-pumped by a voltage of the second harmonic.

CHAPTER VI TRANSIENT BEHAVIOR AND CHARACTERISTICS OF THE HIGH-FIELD DOMAIN IN TRANSFERRED-ELECTRON SEMICONDUCTORS

6.1 INTRODUCTION

A small-signal theory has been applied to transferred-electron diodes to derive a small-signal admittance, and the conditions for current instability and for a negative resistance.[1]-[3] A large-signal theory has been used to analyze stable behavior of a high-field domain in transferred-electron diodes.[4] Theory is not sufficient to understand transient behavior of the domain, which has been investigated mostly by computer analysis.[2], [5] Theoretical work on transient behavior of the domain is required to understand transient phenomena of transferred-electron oscillations, and non-linear and parametric operations of transferred-electron diodes, such as are used in high-speed switching elements, frequency mixers, frequency up-converters, and self-pumped oscillators.[6]-[9]

Quasi-linear equations are used to analyze transient and stable behavior of a high-field domain in transferred-electron diodes. The analysis shows that an equivalent admittance of a domain is represented by a parallel connection of capacitance and conductance which vary with time in the transient state. The equations for the shape of a high-field domain and for the time-constant of the admittance are derived. The width of a high-field domain and the displacement current of diodes are discussed. Numerical examples of characteristics of a high-field domain based on the results of the analysis are given.

It is pointed out that non-linear and parametric operations of transferred-electron diodes can be interpreted by the use of an expression for admittance of the diode in which the effects of rf circuit voltage on the domain are taken into account.

6.2 EQUATIONS FOR DOMAIN

Transient behavior of a high-field domain has been in most cases studied by computer analysis in which the understanding of transient behavior is limited to specified cases reported previously.[2], [5] Only a few papers have studied the growth of the domain in a theoretical analysis.[10], [19] Transient behavior has thus not been sufficiently investigated to provide an understanding of non-linear and parametric phenomena in transferred-electron diodes. In this section quasi-linear differential equations for the domain in a transient state are derived, and in subsequent sections the solutions to the equations are given.

We consider a uniformly-doped bulk semiconductor in which the drift velocity of carriers depends non-linearly on the electric field, such as in GaAs and InP. A bulk semiconductor diode of uniform cross-sectional area A and of length L is considered. As discovered by J. B. Gunn,[11] a disturbance in the field near the cathode contact (the low-voltage side) of a diode grows to a high-field domain when the apllied field to the diode is in the range where the bulk semiconductor shows a negative differential mobility. There are two regions of the field in an oscillating diode: one is a low-field region; the other is a high-field region (customarily called a high-

field domain), as shown in Fig. 6.1(a). The total current density $J(t)$ in the low-field region is given by

$$J(t) = \rho_0 u_0(t) + \varepsilon \frac{\partial}{\partial t} E_0(t) \tag{6.1}$$

where, for convenience in the analysis, the charge of the carriers is assumed positive. The results obtained from the analysis are applicable to n-GaAs and n-InP by changing the sign of the charge. In the low-field region the field $E_0(t)$ is assumed to have no spatial variation which implies by Poisson's equation that the value of the charge density is equal to the value of the charge of the doping concentration ρ_0. In Eq. (6.1), a conduction current is given by the first term where $u_0(t)$ is the drift velocity of the carriers in the low-field region, and a displacement current is given by the second term where ε is the permittivity of the semiconductor. The diffusion current in the low-field region is zero because of spatial uniformity of charge density. The total current density in the high-field domain is given by

$$J(t) = \rho(x, t)u(x, t) + \varepsilon \frac{\partial}{\partial t} E(x, t) - D \frac{\partial}{\partial x} \rho(x, t) \tag{6.2}$$

where the charge denisty ρ, the drift velocity u of carriers, and the electric field E vary not only with time t but also with position x in the high-field domain. In Eq. (6.2) the total current in the high-field domain is obtained by the sum of the conduction, the displacement, and the diffusion currents, respectively, where D is the diffusion coefficient. The term $\rho(\partial D/\partial x)$ is neglected in Eq. (6.2) since it has little effect

on the analysis and complicates physical understanding of the results. The field dependency of the diffusion coefficient is, however, taken into account when the value of the average diffusion coefficient of the domain is computed in Section 6.6. The total current density J is a function of only the time t since total current density is continuous through a diode with a uniform cross-sectional area. The Poisson equation in a high-field domain is

$$\frac{\partial}{\partial x} E(x, t) = \frac{1}{\varepsilon}\left\{\rho(x, t) - \rho_0\right\} \equiv \frac{1}{\varepsilon}\Delta\rho(x, t) \tag{6.3}$$

Using the continuity of total current, and putting Eq. (6.1) equal to Eq. (6.2), we have

$$D\frac{\partial^2}{\partial x^2}\Delta E(x, t) - u(x, t)\frac{\partial}{\partial x}\Delta E(x, t) - \frac{\rho_0\mu_d}{\varepsilon}\Delta E(x, t) = \frac{\partial}{\partial t}\Delta E(x, t) \tag{6.4a}$$

$$\Delta E(x, t) = E(x, t) - E_0(t) \tag{6.4b}$$

$$\mu_d(E, E_0) = \frac{u(E) - u_0(E_0)}{E - E_0} \tag{6.4c}$$

where $\Delta E(x,t)$ is the electric field which is the difference between the fields in the high-field domain and the low-field region, as shown in Fig. 6.1(a). The parameter μ_d has the dimensions of mobility and is considered to be function of the fields E and E_0. It is interesting to notice that Eq. (6.4a) is very similar equation to that for the perturbation in the charge density of a bulk semiconductor examined by the Haynes-Shockley experiment, [12], [13] although in Eq. (6.4a) the diffusion

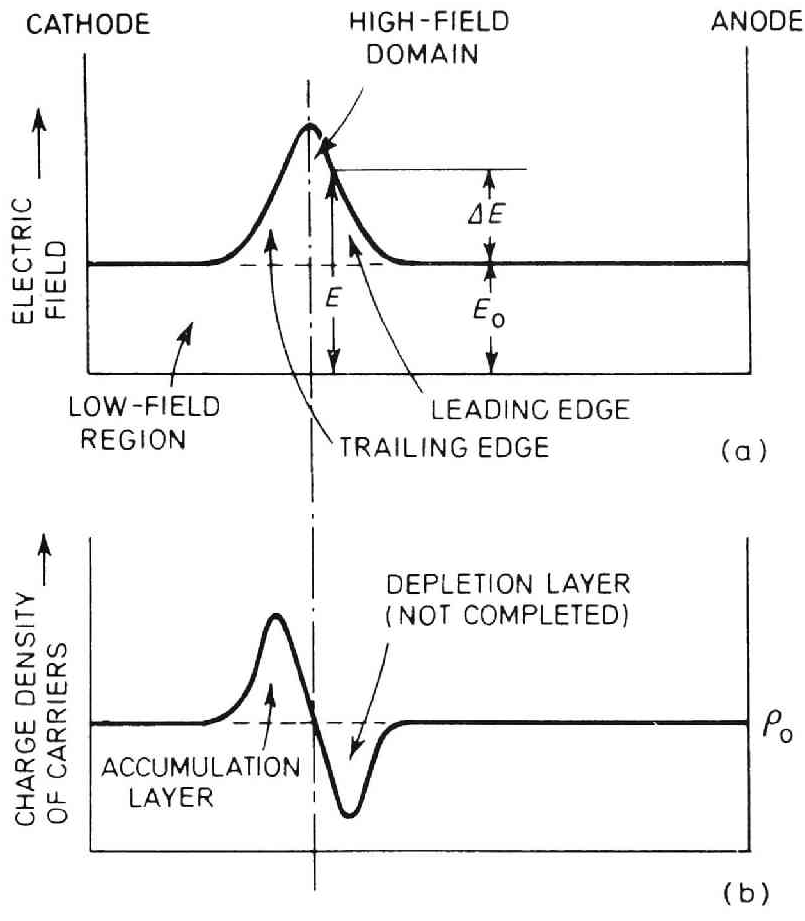

Fig. 6.1 Distribution of electric field (a) and charge density of carriers (b) in transferred-electron diode with fractional depletion of carriers in leading edge.

coefficient and the mobility parameter depend strongly on the field. In Eq. (6.4a), which is the equation for a domain excess field ΔE, the three terms in the left-hand side can be interpreted in the following way: the first term represents the diffusion effect of spreading in width; the second term represents the propagation of the domain excess field ΔE with the velocity $u(x,t)$; and the third term represents change of the domain at the rate of the relaxation time $\varepsilon/\rho_0\mu_d$, growing with

negative μ_d and decaying with positive μ_d. In a semiconductor in which the drift velocity is linearly proportional to the field, a perturbation in the field decays to zero since the mobility given in Eq. (6.4c) is always positive. On the other hand, in a semiconductor which exhibits the transferred-electron effect, the mobility μ_d can be negative as long as the drift velocity $u(E)$ of carriers in the domain is slower than the drift velocity $u_0(E)$ of carriers in the low-field region. Thus a perturbation in the field grows because the slow velocity of carriers in the domain causes a depletion region in the leading edge and an accumulation region in the trailing edge. The mobility μ_d given in Eq. (6.4c) reduces to the differential mobility $(\partial u/\partial E)$ in a small-signal treatment when the difference of the field ΔE tends to the value being considered as a perturbation. In a large-signal treatment, the mobility in the relaxation time is not given by the differential mobility. As long as the mobility μ_d is positive, there is a decay of the domain in diodes even if the differential mobility $(\partial u/\partial E)$ of the carriers in the domain is negative. The decay of the domain, other than at the anode contact (the high-voltage side) of diodes, has been seen in the figures of a high-field domain presented in the flip-page sequence III given by computer analysis.[2]

6.3 TRANSIENT BEHAVIOR OF DOMAIN

The distribution of the charge density of the carriers in a high-field domain is shown in Figs. 6.1(b) and 6.3(b). The carriers are depleted in the leading edge and accumulated in

the trailing edge. The carriers in the leading edge cannot be depleted more than the doping concentration. When the carrier depletion in the leading edge becomes complete, the leading edge spreads in width, as shown in Fig. 6.3(b). For simplicity, the analysis of the domain growth is divided in two parts: the first analyses the transient behavior with a fractional depletion of carriers in the leading edge and does not take into account the effects on the domain growth of the limitation in carrier depletion; the second analyses the transient behavior with a complete depletion of carriers in the leading edge, assuming the replacement of an almost complete depletion by a complete depletion with the same amount of depleted charge.

6.3.1 Growth of Domain With Fractional Depletion

The diffusion coefficient D, the drift velocity u, and the mobility μ_d in Eq. (6.4a) depend strongly on the field. They could be assumed nearly constant, however, when Eq. (6.4a) is applied in a sufficiently short time that their variations are small enough to neglect. The coefficients for the subsequent short time can be obtained from the field distribution for the previous short time since the coefficients are functions of the field. By postulating an initial disturbance in the field, we could study transient behavior of the domain in successive short time intervals until the domain reaches a stable state. By transferring Eq. (6.4a) to the coordinate

$$x' = x - ut \tag{6.5}$$

we analyse the field in the coordinates moving with the carrier velocity u in the domain and we obtain

$$D\frac{\partial^2}{\partial x'^2}\Delta E(x', t)-\frac{\rho_0\mu_d}{\varepsilon}\Delta E(x', t)=\frac{\partial}{\partial t}\Delta E(x', t) \tag{6.6}$$

The field in an initial disturbance is assumed to have a Gaussian distribution which is expressed by

$$\Delta E(x, 0)=\Delta E(0)\exp\left[-\frac{(x-x_{00})^2}{k}\right] \tag{6.7}$$

where $\Delta E(0)$ is an initial amplitude of the field, x_{00} is the position of the disturbance occuring near the cathode $x = 0$, and k is such a small value of the length parameter that the value of the excess field ΔE is assumed zero at the cathode in the analysis. The potential in an initial disturbance is obtained by integrating Eq. (6.7) from the cathode $x = 0$ to the anode $x = L$, we have

$$\Delta V(0)=\sqrt{k\pi}\,\Delta E(0) \tag{6.8}$$

where zero excess fields at the cathode and the anode are assumed. From Eq. (6.6) the field distribution in the domain is obtained as

$$\Delta E(x', t)=\frac{\Delta V(0)}{\sqrt{k\pi+4\pi Dt}}\exp\left[-\frac{\rho_0\mu_d}{\varepsilon}t-\frac{(x'-x_0)^2}{k+4Dt}\right] \tag{6.9}$$

which satisfies the initial disturbance given by Eq. (6.7). In Eq. (6.9) the term $\exp[-(x'-x_0)^2/(k+4Dt)]$ describes the Gaussian distribtution of the field in the domain, the term $\exp(-\rho_0\mu_d t/\varepsilon)$ describes the domain growth at the rate of the inverse relaxation

time $(\rho_0\mu_d/\varepsilon)$, when the mobility μ_d is negative, and the term $\sqrt{k\pi+4\pi Dt}$ describes the spread in width with time by the diffusion effect. The integration of the field distribution gives the potential of the domain,

$$\Delta V(t) = \Delta V(0)\exp\left[-\frac{\rho_0\mu_d}{\varepsilon}t\right] = \sqrt{k\pi+4\pi Dt}\cdot\Delta E(x_0, t) \tag{6.10}$$

where $\Delta E(x_0, t)$ is the maximum field in the domain. The expression of Eq. (6.6) in terms of the potential rather than the field becomes

$$\left(\rho_0\mu_d+\frac{2\varepsilon D}{k+4Dt}\right)\frac{\Delta V(t)}{\sqrt{k\pi+4\pi Dt}} + \frac{\partial}{\partial t}\left\{\frac{\varepsilon}{\sqrt{k\pi+4\pi Dt}}\cdot\Delta V(t)\right\} = 0 \tag{6.11}$$

It can be seen that the admittance of the domain of the excess field can be represented by the parallel connection of the conductance

$$G_d(t) = \left(\rho_0\mu_d+\frac{2\varepsilon D}{k+4Dt}\right)\frac{1}{\sqrt{k\pi+4\pi Dt}} \tag{6.12}$$

and the capacitance

$$C_d(t) = \frac{\varepsilon}{\sqrt{k\pi+4\pi Dt}} \tag{6.13}$$

both of which show time variation. It is seen in Eq. (6.11) that the total current is zero in the domain. The term $\sqrt{(k\pi+4\pi Dt)}$ in Eqs. (6.12) and (6.13) is the effective length of the domain, as can be understood in Eq. (6.10), where it appears as the ratio of the potential $\Delta V(t)$ to the field $\Delta E(x_0, t)$.

The term $\rho_0\mu_d$ is a negative conductivity resulting from the negative mobility, and the term $2\varepsilon D/(k+4Dt)$ is positive conductivity resulting from the diffusion effect. It should be noticed that the time variation of the effective length $\sqrt{(k\pi+4\pi Dt)}$ depends on the relative value of the initial length $\sqrt{(k\pi)}$ to the variable length $\sqrt{(k\pi Dt)}$; large variation of the effective length or of the capacitance could not be expected if $k\pi \gg 4\pi Dt$ for the time period being considered. Substituting Eq. (6.9) into Poisson's equation (6.3), we obtain the distribution of the charge density of the carriers in the domain:

$$\Delta\rho(x', t) = \frac{2\varepsilon(x'-x_0)}{k+4Dt}\Delta E(x', t) \tag{6.14}$$

which is shown in Fig. 6.1(b). The integration of the charge density in the leading or trailing edge gives the charge $\Delta Q(t) = \varepsilon\Delta V(t)/\sqrt{(k\pi+4\pi Dt)}$. Using the definition of the capacitance $C_d(t) = \Delta Q(t)/\Delta V(t)$, we obtain the domain capacitance already derived in Eq. (6.13). The differential capacitance, defined as $C_d'(t) = \partial\{\Delta Q(t)\}/\partial\{\Delta V(t)\}$, is often of interest and is in the present case given by $C_d'(t) = C_d(t)$ since the charge $Q(t)$ is a linear function of the voltage $\Delta V(t)$.

The admittance of the domain can be interpreted in Fig. 6.2 where the charge distributions of the carriers are shown. With the domain growing, the carriers are being depleted in the leading edge and accumulated in the trailing edge. There are, in Fig. 6.2(b), larger depleted and accumulated regions than in Fig. 6.2(a). Although in practice the accumulation is formed by carriers coming behind the trailing edge of the domain, and the depletion by carriers moving forward from the leading edge,

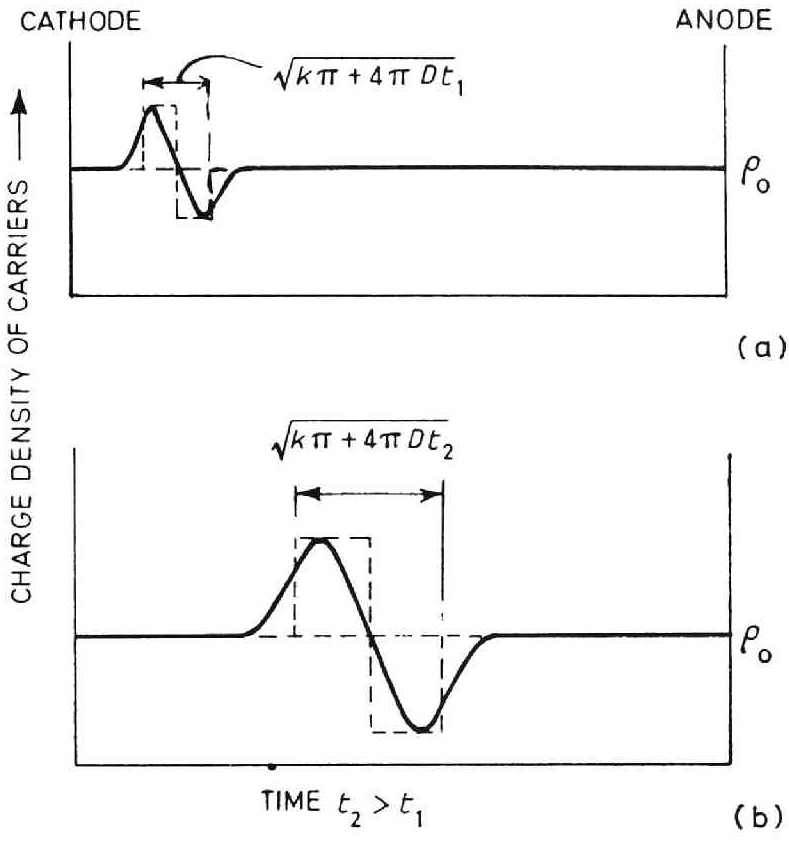

Fig. 6.2 Distribution of charge density of carriers where the area under the dotted line is equal to the area under the solid line, and thus $\sqrt{k\pi+4\pi Dt}$ can be considered as effective width of domain.

it could be considered that both the depletion and the accumulation are formed by a virtual transfer from the leading edge to the trailing edge. There is in the domain an effective velocity component directed from the leading edge to the trailing edge whereas the total carrier in the diode moves from the cathode contact to the anode. Negative conductance of the domain thus can be considered as resulting from the inverse directed velocity component of the carriers in the domain. Positive conductance of the domain, on the other hand, results from the diffusion velocity directed from the trailing edge to

the leading since the carrier density in the trailing edge is larger than that in the leading edge. The existence of the capacitance in the domain can be interpreted by saying that the carrier distribution of the domain corresponds to the charge distribution of the space-charge region in a p-n diode where the width of the region is given by $\sqrt{(k\pi+4\pi Dt)}$.

On applying a bias voltage V_b to a diode of length L, we have

$$V_b = E_b L + \Delta V(0) \quad . \tag{6.15}$$

where E_b is the bias field of the diode. After an initial potential $\Delta V(0)$ grows up to $\Delta V(t)$ in the diode, the electric field of the low-field region decreases from E_b to $E_0(t)$ which satisfies

$$V_b \cong E_0(t)L + \Delta V(t) \tag{6.16}$$

where the rf circuit voltage induced by the diode is assumed small compared with the dc bias voltage V_b. From Eqs. (6.15) and (6.16), we obtain the field of the low-field region

$$E_0(t) = E_b - \frac{1}{L}\{\Delta V(t) - \Delta V(0)\} \tag{6.17}$$

Substituting the field $E_0(t)$ into the equation:

$$J_0(t) = \rho_0 \mu_L E_0(t) + \varepsilon \frac{\partial}{\partial t} E_0(t) \tag{6.18}$$

we can calculate the total current density of the diode. In Eq. (6.18), the conduction current is given by the first term where μ_L is the carrier mobility in the low-field region, and the displacement current is given by the second term.

6.3.2 Growth of Domain With Complete Depletion

The leading edge spreads in width as the charge depletion in the leading edge approaches completion. For simplicity of analysis, an almost complete depletion is replaced by a complete depletion with the same amount of depleted charge. The accumulation region is assumed to grow continuously according to the results obtained in Section 6.3.1. The field distribution of the trailing edge $\Delta E_1(x',t)$ is thus given by Eq. (6.9). The subscript 1 of ΔE_1 denotes the left-hand side of the domain, but not the leading edge which is in the right-hand side of the domain . The field distribution of the leading edge $\Delta E_r(x',t)$ is obtained by solving Poisson's equation and applying the condition of field continuity, $E_1(x_0,t) = E_r(x_0,t)$, at $x' = x_0$ which is the boundary between the trailing and leading edges as shown in Fig. 6.3.

$$\Delta E_r(x',t) = -\frac{\rho_0}{\varepsilon}(x'-x_0) + \frac{\Delta V(0)}{\sqrt{k\pi+4\pi Dt}} \exp\left[-\frac{\rho_0\mu_d}{\varepsilon}t\right] \tag{6.19}$$

The field distribution of the trailing edge is mainly affected by the diffusion effect; the field distribution of the leading edge is mainly affected by charge of the impurity concentration, ρ_0. The width $(w' - x_0)$ of a complete depletion region is derived from the equation $\Delta E_r(w',t) = 0$ which represents zero excess field at the edge $x' = w'$ of the depletion region.

$$w'-x_0 = \frac{\varepsilon\Delta V(0)}{\rho_0\sqrt{k\pi+4\pi Dt}} \exp\left[-\frac{\rho_0\mu_d}{\varepsilon}t\right] \tag{6.20}$$

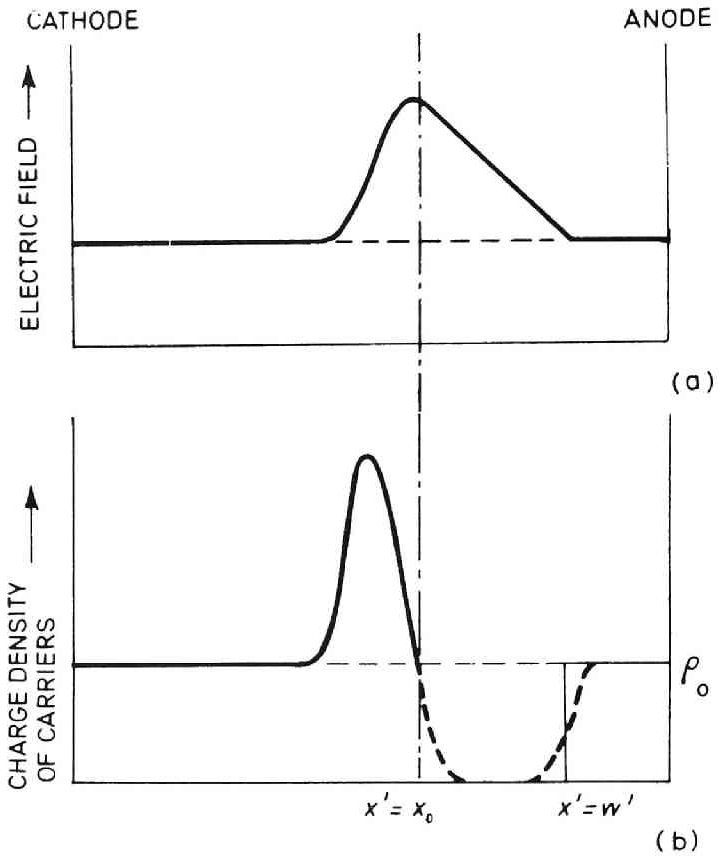

Fig. 6.3 Distribution of electric field (a) and charge density of carriers (b) in transferred-electron diode with complete depletion of carriers in leading edge.

This shows that the width of a complete depletion region spreads with growth of the maximum field of the domain,

$$\Delta E(x_0, t) = \Delta V(0)\exp(-\rho_0\mu_d t/\varepsilon)/\sqrt{k\pi + 4\pi Dt}.$$

The potential of a domain is obtained by the integration of a domain of the field $\Delta E_l(x', t)$ from the cathode contact to $x' = x_0$ and the integration of the field $\Delta E_r(x', t)$ from $x' = x_0$ to $x' = w'$.

$$\Delta V(t) = \frac{\Delta V(0)}{2} \exp\left[-\frac{\rho_0 \mu_d}{\varepsilon} t\right] + \frac{\varepsilon}{2\rho_0} \{\Delta E(x_0, t)\}^2 \qquad (6.21)$$

where the first term presents the potential of the trailing edge and the second the potential of the leading edge. With sufficient growth of the domain, the potential of the leading edge becomes larger than the potential of the trailing edge. Thus the potential, with sufficient growth of the domain, becomes proportional to the square of the maximum excess field of the domain, $\Delta E(x_0, t)$. This proportionality has been observed in the experiments on the shape of travelling domains in GaAs by J. B. Gunn [14] and the experiments on high-field dipole domains in GaAs by I. Kuru *et al.* [15] The charge of the domain, $\Delta Q(t)$, is obtained by the assumption of charge neutrality in the diode:

$$\Delta Q(t) = \rho_0(w' - x_0) = \varepsilon \Delta E(x_0, t) \qquad (6.22)$$

With sufficient growth of the domain, the charge $\Delta Q(t)$ is proportional to the square root of the domain voltage, $\sqrt{\Delta V(t)} \cong \sqrt{\varepsilon/2\rho_0} \cdot \Delta E(x_0, t)$, which has been measured experimentally. [14] The application of the definitions of the capacitance and the differential capacitance to Eqs. (6.21) and (6.22) gives

$$C_d(t) = \frac{\Delta Q(t)}{\Delta V(t)} = \frac{2\varepsilon}{\sqrt{k\pi + 4\pi D t} + (w' - x_0)} \qquad (6.23a)$$

and

$$C'_d(t) = \frac{\partial \Delta Q(t)}{\partial \Delta V(t)} = \frac{\varepsilon}{\frac{1}{2}\sqrt{k\pi + 4\pi D t} + (w' - x_0)} \qquad (6.23b)$$

which show that the values of these capacitances are decreasing

with time. The differential capacitance $C_d'(t)$ is different from the capacitance $C_d(t)$ since the charge is not a linear function of the voltage $\Delta V(t)$. In the differential capacitance, the first term of the denominator represents the effective width of the accumulation region and the second the width of the depletion region. If, as obtained in Section 6.3.1, the total current in the domain is assumed to be zero here,

$$G_d(t).\Delta V(t)+\frac{\partial}{\partial}\{C_d(t).\Delta V(t)\}=0, \tag{6.24}$$

we can derive the conductance $G_d(t)$:

$$G_d(t)=\left(\rho_0\mu_d+\frac{2\varepsilon D}{k+4D}\right)\times\frac{2}{\sqrt{k\pi+4\pi Dt}+(w'-x_0)} \tag{6.25}$$

where the denominator has length dimensions and the same value as that in the capacitance $C_d(t)$; and where the term $\rho_0\mu_d$ represents negative conductivity resulting from the negative mobility and the term $2\varepsilon D/(k+4Dt)$ represents positive conductivity resulting from the diffusion effect. The fields of the low-field region $E_0(t)$ and the total current density of the diode $J_0(t)$ are calculated by Eqs. (6.17) and (6.18) given in Section 6.3.1.

When the domain reaches a steady state, it can be expected for the domain not to vary with time. There is no displacement current in the domain , which by Eq. (6.24) implies zero conductance of the domain. In a steady state, no effective transfer of the carriers occurs between the leading and trailing edges. The admittance of the domain in a steady state is repre-

sented by the capacitance determined by the carrier distributions of the leading and trailing edges.

6.3.3 Extinction of Domain at the Anode Contact

The carrier distribution of the metal near the anode contact is disturbed by the arrival of the depletion region of the domain. The disturbances are extinguished at the rate of the dielectric relaxation time ε/σ_m where σ_m is the conductivity of the metal. As the conductivity of the metal is large, the disturbances would be assumed to be extinguished at the instant the depletion region of the domain arrives at the anode contact. The transient behavior of the domain being extinguished at the anode contact is studied in this section by a simple analysis in which zero relaxation time of the metal is assumed. At the time t after the depletion region arrives at the anode contact, the width of the depletion region is given by

$$(w_s' - x_0 - \mu_L E_0(t)t),$$

where $(w_s' - x_0)$ is the width of the domain in the steady state and the domain velocity is approximated by the velocity of the carriers in the low-field region, $\mu_L E_0(t)$. The neutrality of total charge in the diode implies

$$\frac{\varepsilon \Delta V(0)}{\sqrt{k\pi + 4\pi D t'}} \exp\left[-\frac{\rho_0 \mu_d}{\varepsilon} t'\right] = \rho_0 \{w_s' - x_0 - \mu_L E_0(t)t\} \tag{6.26}$$

where the left-hand side gives the charge in the accumulation region and the right the charge in the depletion region. In Eq. (6.26), t' denotes a time parameter which decreases with

increasing values of the time t because the accumulation region must decrease with the time t. The bias voltage V_b is expressed by

$$V_b = E_0(t)L + \frac{\Delta V(0)}{2}\exp\left[-\frac{\rho_0\mu_d}{\varepsilon}t'\right] + \\ + \frac{\rho_0}{2\varepsilon}\{w_s' - x_0 - \mu_L E_0(t)t\}^2 \qquad (6.27)$$

where the rf circuit voltage is assumed small compared with the dc bias voltage V_b. In Eq. (6.27) the first, second, and third terms represent the potentials of the low-field region, of the trailing edge, of the leading edge, respectively. The field $E_0(t)$ and the time parameter t' are obtained from Eqs. (6.26) and (6.27) at a given time t. The use of the potential of the domain and the charge given by Eq. (6.26) with the definitions for capacitance and differential cpapcitance gives the domain capacitance:

$$C_d(t) = \frac{2\varepsilon}{\sqrt{k\pi + 4\pi D t'} + \{w_s' - x_0 - \mu_L E_0(t)t\}} \qquad (6.28a)$$

and the differential capacitance of the domain:

$$C_d'(t) = \frac{\varepsilon}{\frac{1}{2}\sqrt{k\pi + 4\pi D t'} + \{w_s' - x_0 - \mu_L E_0(t)t\}} \qquad (6.28b)$$

The first and second terms in the denominator of $C_d'(t)$ are respectively the effective widths of the trailing and the leading edges. As these terms decrease with time the capacitances $C_d(t)$ and $C_d'(t)$ of the domain being extinguished at the anode contact, increase with time. The conductance is obtained from Eq. (6.24); the width of the domain is given by the denominator of Eq. (6.28b); the field distribution of the trailing edge is given by Eq. (6. 9),

using the time parameter t' in place of the time t; the field distribution of the leading edge is given by

$$\Delta E_r(x', t) = -\frac{\rho_0}{\varepsilon}\{w_s' - x_0 - \mu_L E_0(t)t\} + \\ + \frac{\Delta V(0)}{\sqrt{k\pi + 4\pi D t'}} \exp\left[-\frac{\rho_0 \mu_d}{\varepsilon} t'\right];$$

the domain potential is given by the second and third terms in Eq. (6.27); and the total current density is obtained from Eq. (6.18). The time for the domain to be extiguished at the anode contact can be approximated by the time when the width of the domain reduces to the width of the initial disturbance, $\sqrt{(k\pi)}$. The time obtained from this calculation would not be an accurate value of the time for extinction, but could give an approximate value of it.

6.4 DOMAIN CHARACTERISTICS

6.4.1 Domain Shape

Two types of domain shape could be considered when the domain reaches a steady state: one with a fractional depletion in the leading edge; the other with a complete depletion in the leading edge. As shown in Fig. 6.1(a), a domain with a fractional depletion is in the shape of a Gaussian distribution which is symmetrical with respect to the position of maximum field. The shape of a domain with a complete depletion is asymmetrical as shown in Fig. 6.3(a). The potential of a domain with a complete depletion is generally larger than that of a domain with a fractional depletion because it reaches a steady state through the process of growth of a domain with a fractional depletion.

It can be said that the shape of the domain with a relatively small potential is a symmetrical triangle and that the shape of the domain with a relatively large potential is an asymmetrical triangle. These shapes have been observed in experiments.[14]

6.4.2 Domain Excess Potential

The approximate value of the potential of a domain in a steady state is calculated by a simple equation. Neglecting an initial potential $\Delta V(0)$ in Eqs. (6.16) and (6.17), we obtain

$$\frac{\Delta V(t)}{V_b} = 1 - \frac{E_0}{E_b} \tag{6.29}$$

in which the value of $\Delta V(t)/V_b$ is 54 % when the threshold field 3.25 kV/cm is used for the bias field E_b and a minimum sustaining field (about 1.5 kV/cm) is used for the field E_0 in the low-field region.

6.4.3 Time-Constant of the Domain Admittance

The time-constant of the admittance of the domain with a fractional depletion is derived by using Eqs. (6.12) and (6.13).

$$\frac{1}{\tau_c} = \frac{G_d(t)}{C_d(t)} = \frac{\rho_0 \mu_d}{\varepsilon} + \frac{2D}{k+4Dt} \tag{6.30}$$

It is interesting to see that the time-constant of the domain admittance relates closely to the dielectric relaxation time. As μ_d is negative for the domain growth, the second term in Eq. (6.30) indicates the reduction of the growth rate by the diffusion effect. The time-constant of the admittance of the domain

with a complete depletion is derived from Eqs. (6.23a) and (6.25), and it is given by the same expression as that of Eq. (6.30).

6.5 NON-LINEAR OR PARAMETRIC OPERATION OF DIODE

A time-varying admittance is derived for a diode which is treated as an active element of a circuit. When the diode is biased by the direct voltage V_b and the rf circuit voltage $\Delta V_c(t)$, the voltage equation (6.16) is rewritten as

$$V_b + \Delta V_c(t) = E_0(t)L + \Delta V(t) \tag{6.31}$$

where the rf circuit voltage can either be induced in the circuit by the domain voltage or introduced as an applied rf voltage, not necessarily of the same frequency or variation as the domain voltage. Substituting $E_0(t)$ into the total current $I(t) = A \cdot J(t)$ where A is the cross-sectional area of a diode and $J(t)$ is the total current density given by Eq. (6.1), we obtain

$$\Delta I(t) = G_p(t) \cdot \Delta V_c(t) + \frac{\partial}{\partial t}\{C_p(t) \cdot \Delta V_c(t)\} \tag{6.32a}$$

$$\Delta I(t) = I_0(t) - I, \quad I = \frac{1}{T}\int_0^T I_0(t)\mathrm{d}t \tag{6.32b}$$

$$G_p(t) = \frac{G_0 \cdot V_b - I}{\Delta V_c(t)} + G_0\left\{1 - \frac{\Delta V(t)}{\Delta V_c(t)}\right\} \tag{6.32c}$$

$$C_p(t) = C_0\left\{1 - \frac{\Delta V(t)}{\Delta V_c(t)}\right\} \tag{6.32d}$$

where T is the period of the domain transit in a diode, G_0 is

a low-field conductance given by $A\rho_0\mu_L/L$, C_0 is the geometrical capacitance given by $A\varepsilon/L$, and $\Delta I(t)$ is the rf current obtained by substracting the dc component I from the total current $I_0(t)$. It is seen in Eq. (6.32a) that the terms $G_p(t)$ and $C_p(t)$ could be considered to be the conductance and the capacitance of the diode which is treated as an active element of a circuit. The domain voltage $\Delta V(t)$ in the conductance $G_p(t)$ and capacitance $C_p(t)$ varies not only with the frequency determined by the length of the diode but also with the frequency of the circuit voltage which affects the domain growth non-linearly. The conductance $G_p(t)$ and the capacitance $C_p(t)$, which vary non-linearly with respect to the applied rf voltage and parametrically with respect to time, allow interpretation of the non-linear or parametric operation of diodes when used as frequency mixers, frequency up-converters and self-pumped oscillators.

6.6 NUMERICAL EXAMPLES OF DOMAIN CHARACTERISTICS

Transient and stable characteristics of domains are shown in numerical examples calculated by the analytical results obtained in previous sections where the diffusion coefficient D, the drift velocity u, and the mobility μ_d have been assumed approximately constant in a very short time Δt. The growth of the disturbance for the time $t = \Delta t$, from $t = 0$ to $t = \Delta t$, can be calculated by using an initial disturbance in field and potential, and initial values of the diffusion D, the velocity u and the mobility μ_d. In a subsequent time interval from $t = \Delta t$ to $t = 2\Delta t$, the growth of the disturbance is calculated by using the coefficients which are averaged with respect to the carrier density at time $t = \Delta t$; for

example,

$$\bar{\mu}_d = \frac{\int_{E_o}^{E_m} \mu_d \cdot (\rho_l + \rho_r) dE}{\int_{E_o}^{E_m} (\rho_l + \rho_r) dE} \tag{6.33}$$

where E_m is a maximum field in a high-field domain, and ρ_l and ρ_r are the distributions of the charge density expressed in terms of the electric field. The subscripts l and r denote the left-hand side (trailing edge) and the right-hand side (leading edge) of the domain, respectively. When the charge distributions are symmetrical as shown in Fig. 6.1(b) and written as $\rho_l = \rho_0 + \Delta\rho(E)$ and $\rho_r = \rho_0 - \Delta\rho(E)$, the average mobility is given by

$$\bar{\mu}_d = \int_{E_o}^{E_m} \mu_d dE/(E_m - E_0) \tag{6.34}$$

In a domain with a complete depletion region, the leading edge is not taken into account for evaluating the average mobility $\bar{\mu}_d$ since there are no carriers in the leading edge: $\rho_r = 0$. The mobility of the region between a low-field E_0 and the threshold field E_T in a domain would act to suppress the growth of the domain because the mobility in this region reduces the absolute value of a negative mobility μ_d in the evaluation of Eq. (6.33). Thus the average mobility given by Eq. (6.33) takes into consideration such effects as the lack of carriers in the leading edge and the suppression of domain growth by the low-field mobility in the domain. The velocity-field characteristic shown in Fig. 6.4, which is approximated from that derived theoretically by P. N. Butcher and W. Fawcett, [16] is used in making the calculations. The field dependency of the diffusion coefficient is also taken into account in the calcu-

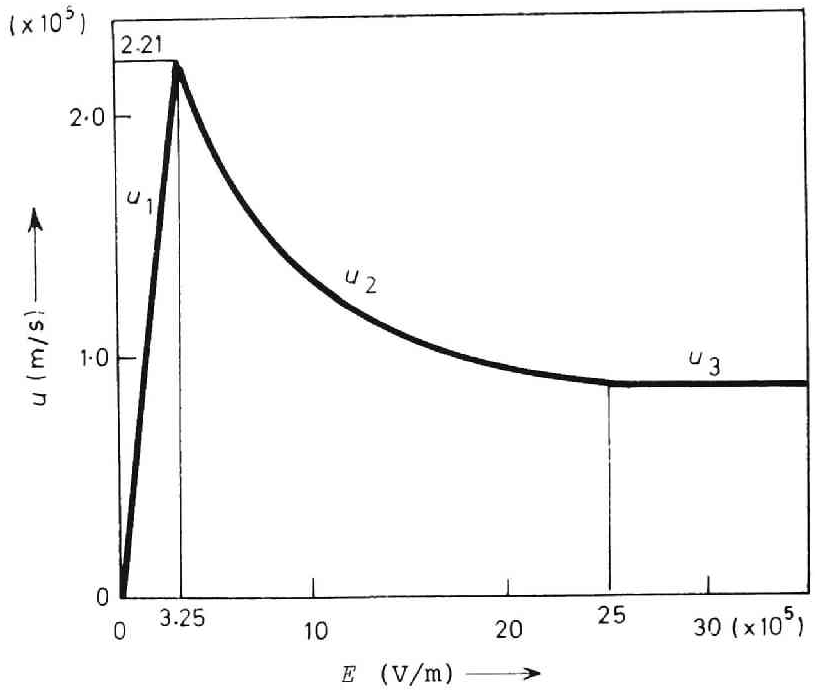

$U_1 = 0.68$ $\qquad U_2 = \dfrac{1}{A + B \cdot E} + C$

$U_3 = 0.87$ $\qquad A = 0.2442381 \times 10^{-5}$

U = DRIFT VELOCITY IN m/s $\qquad B = 0.108 \times 10^{-10}$

E = ELECTRIC FIELD IN V/m $\qquad C = 0.53 \times 10^{5}$

Fig. 6.4 Velocity-field characteristic used in computation.

lations, and the diffusion coefficient-field characteristic approximated from that given theoretically by P. N. Butcher *et al.*[17] is used. The average diffusion is evaluated by the technique of Eq. (6.33).

The potential corresponding to thermal energy at room temperature, 0.025 V, is assumed as the value of the initial potential $\Delta V(0)$. It is generally considered[18] that significant departures from electrical neutrality are not found over dis-

tances greater than about four or five times the Debye length L_d. Thus we could choose five times the Debye length as an initial value of the effective width of the domain, $\sqrt{k\pi}$. It could be understood for uniformly-doped semiconductors that the values of $\Delta V(0) = 0.025$ V and $\sqrt{k\pi} = 5L_D$ were determined by one of the methods to decide what are initial disturbances in theoretical analysis. In actual cases of the transferred-electron diodes, initial disturbances could be caused, for example, by non-uniformity in doping and non-ohmic characteristics of the cathode contact.

The impurity concentration of 2.0×10^{20} m^{-3} and a low-field resistivity of 4.6 ohm-cm are used in the calculations of transient and stable characteristics of domains in transferred-electron diodes. Numerical examples of domain characteristics are shown in Figs. 6.5 - 6.7, for three different values of the product $n_0 L$, the time for the domain growth is taken as the time from the initial perturbation until the field of the domain stops increasing. The value of t/T in the abscissa of the figures indicates the ratio of the time t to the period T, which is the transit time of the domain through the sample length with average velocity 10^5 m/s.

It can be seen in Figs. 6.5 - 6.7 that the capacitance of a domain decreases during domain growth because the effective width of the domain is spreaded by the diffusion effect. It can also be seen that a negative conductance of domain is large at the beginning of the domain growth and then decreases during growth of a domain. The domain growth in a diode always accompanies these variations of the capacitance and the conductance. Larger

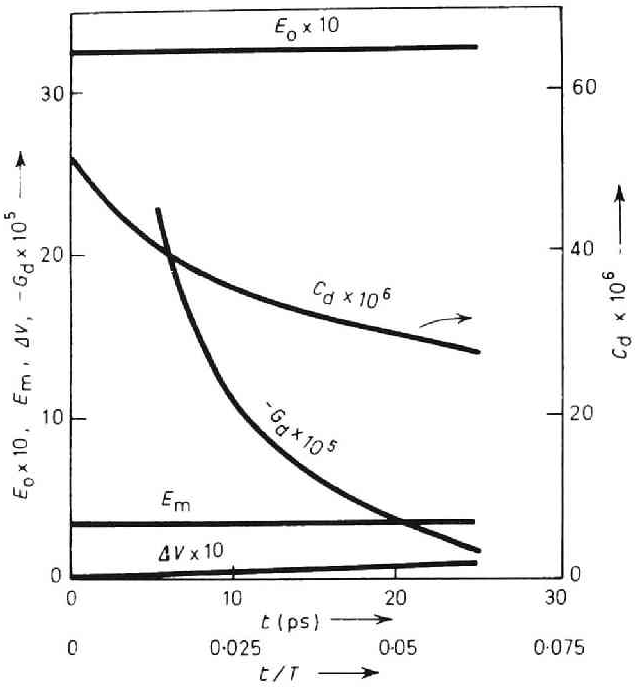

E_0 FIELD OUTSIDE DOMAIN IN kV/cm

E_m MAXIMUM FIELD OF DOMAIN IN kV/cm

ΔV POTENTIAL OF DOMAIN IN VOLTS

C_d CPAPACITANCE OF DOMAIN IN F/m^2

G_d CONDUCTANCE OF DOMAIN IN Ω^{-1}/m

Fig. 6.5 Transient characteristics of domain growing in diode with $n_0 = 2.0 \times 10^{20}$ m^{-3} and $L = 40$ μm ($n_0 L = 0.8 \times 10^{12}$ cm^{-2}) and biased at threshold.

variations in the fields, the potential, and the admittance of a domain are observed with larger values of the product $n_0 L$. The discontinuity appearing in the variations of the capacitance and the conductance in Fig. 6.7 is attributed to the abrupt

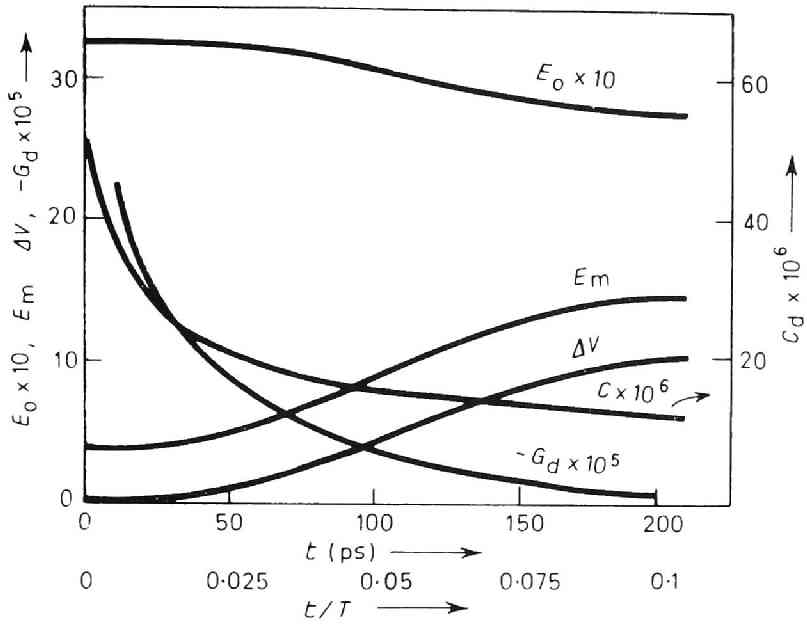

Fig. 6.6 Transient characteristics of domain growing in diode with $n_0 = 2.0 \times 10^{20}$ m^{-3} and $L = 200$ μm ($n_0 L = 4 \times 10^{12}$ cm^{-2}) and biased at threshold. E_0, E_m, ΔV, G_d and C_d are in the same units as in Fig. 6.5.

change of the effective length of the domain, resulting from the assumption of the replacement of an almost depleted region in the leading edge by a completely depleted region.

Characteristics of domains in a steady state are summarized in Table 6.1. It is understood in Table 6.1 that the value of the time for the domain growth ranges between 5 and 10 % of the period of the transit-time oscillation of the diode and thus a long time is required to achieve a steady state in a long sample. The potentials of domains are less than 54 % of the bias voltage which was the percentage obtained in Section 4.2 as the maximum value of the potential in the domain of a diode biased at the threshold field. The displacement current in a sample is much

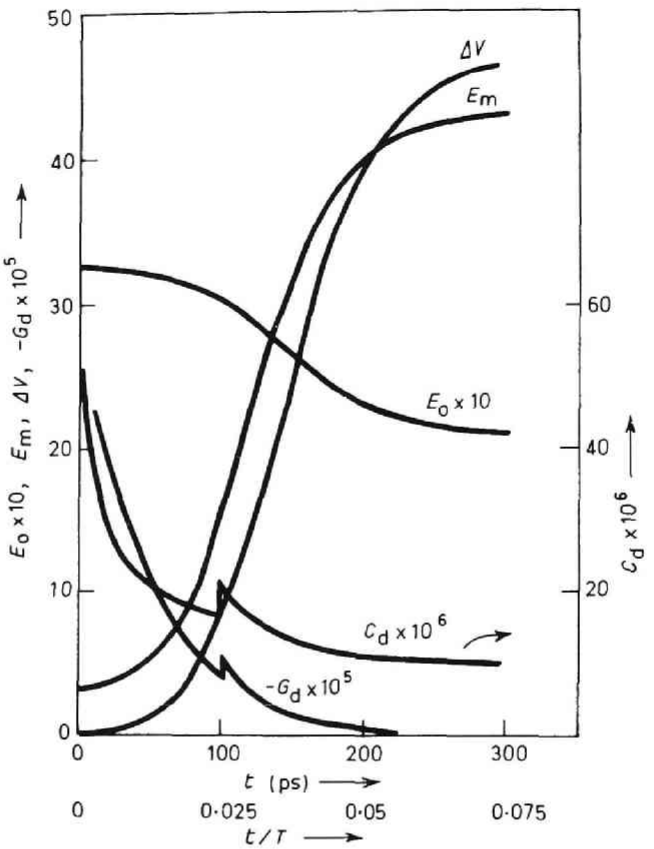

Fig. 6.7 Transient characteristics of domain growing in diode with $n_0 = 2.0 \times 10^{20}$ m^{-3} and $L = 400$ μm ($n_0 L = 8 \times 10^{12}$ cm^{-2}) and biased at threshold. E_0, E_m, ΔV, G_d and C_d are in the same units as in Fig. 6.5.

less than the conduction current. The variation of the total current in a sample biased at the threshold field is approximated by the variation of the electric field outside the domain, as shown in Figs. 6.5 - 6.7. A small capacitance accompanies a large domain potential since the domain grows with spreading width of the domain by the diffusion effect. The width of the

Table 6.1 Characteristics of domain when it reaches a steady state. Diodes are biased at threshold.

		Length of diode μm			
		40	200	400	600
n_0L	cm^{-2}	$0{\cdot}8\times10^{12}$	4×10^{12}	8×10^{12}	12×10^{12}
Time for domain growth	ps	25	210	300	340
Time for domain growth/period of oscillation		0·063	0·11	0·075	0·057
Maximum field of domain	kV/cm	3·4	14	43	58
Potential of domain	volt	0·08	10	46	77
Potential of domain/bias voltage		0·0062	0·16	0·35	0·40
Current density	A/m^2	$7{\cdot}0\times10^{6}$	$5{\cdot}9\times10^{6}$	$4{\cdot}6\times10^{6}$	$4{\cdot}3\times10^{6}$
Displacement current/conduction current		$0{\cdot}65\times10^{-1}$	$1{\cdot}7\times10^{-1}$	$0{\cdot}084\times10^{-1}$	$0{\cdot}66\times10^{-1}$
Capacitance per unit area	F/m^2	27×10^{-10}	12×10^{-10}	$9{\cdot}8\times10^{-10}$	$8{\cdot}0\times10^{-10}$
Effective width of domain	μm	4·1	9·1	18	23
Effective width of domain/length of diode		0·10	0·046	0·045	0·038
Accumulation width/depletion width		1	1	0·3	0·21

$n_0 = 2.0 \times 10^{20}\ m^{-3}$

The ratios of the displacement current of the conduction current are given just before the arrival at a steady state.

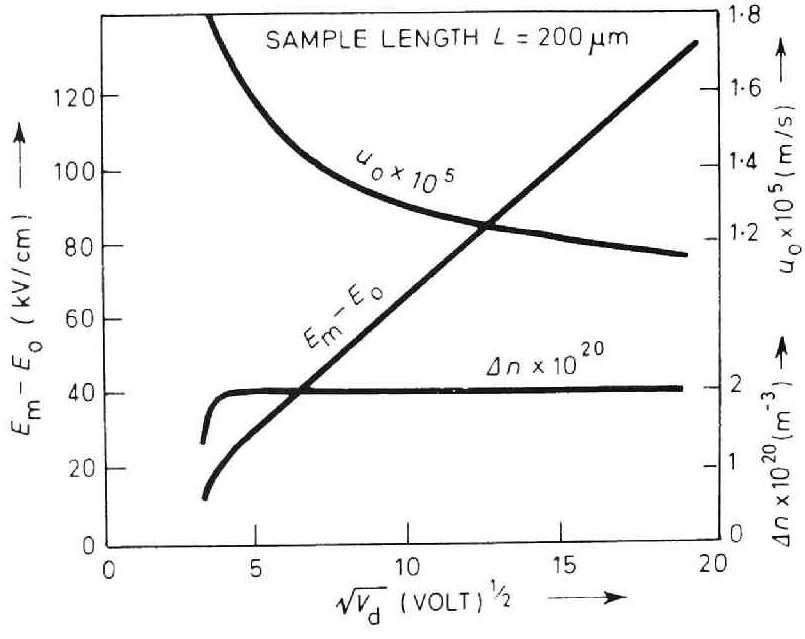

Fig. 6.8 Theoretical variations of carrier velocity u_0 outside domain, excess field $(E_m - E_0)$ of domain, and ionized impurity density $\Delta n = \Delta\rho/q$ appearing in the leading depleted region, plotted as functions of the square root of domain voltage $\sqrt{V_D}$. Note different scales and zeros in each quantity.

leading edge until complete depletion appears in the leading edge, then the width of the leading edge becomes large compared with the width of the trailing edge. The ratio of the accumulation width to the depletion width becomes small, as shown in the last row in Table 6.1.

The characteristics of a domain at a steady state are shown in Fig. 6.8 where the analytical results obtained in Sections 6.2 and 6.3 are applied to a diode of $n_0 = 2.0 \times 10^{20}$ m^{-3} and $L =$ 200 μm at various applied bias voltages. The voltages are assumed to bias the diode instantaneously beyond the threshold.

The characteristics shown in Fig. 6.8 are qualitatively in good agreement with the experimental data measured by the capacitive probe techniques.[14] The domain excess field $(E_m - E_0)$ is linearly proportional to the square root of the domain voltage, $\sqrt{V_D}$. The carriers in the leading edge are almost depleted, except when the domain field and potential are relatively small. Outside the domain the carrier velocity u_0, which is approximately equal to the domain velocity at a steady state, decreases with the increase of domain voltage or domain field. The decrease of the domain velocity can be understood by the negative differential characteristic shown in Fig. 6.4 which implies slower velocity at higher field. Quantitative agreement can be obtained by the use of slightly different initial conditions and velocity-field characteristic in the computation since the trends of the variations given in Fig. 6.8 are the same as those measured experimentally.[14]

The time for domain extinction at the anode can be roughly estimated by the ratio of the domain width to the average velocity. In Table 6.1, the domain width is 18 μm for the diode, biased at the threshold, with $n_0 = 2.0 \times 10^{20}$ m^{-3} and $L = 400$ μm. The time for domain extinction is 180 ps when the average velocity is assumed to be 10^5 m/s. Using the analytical results obtained in Section 6.3.3, we obtain in Fig. 6.9, transient characteristics of domain being extinguished at the anode. The time chosen for the extinction is from the arrival of the edge of the domain at the anode to the reduction of the domain width to the width of the initial perturbation. In Fig. 6.9 we see that the time for the extinction is 63 ps, which is shorter than

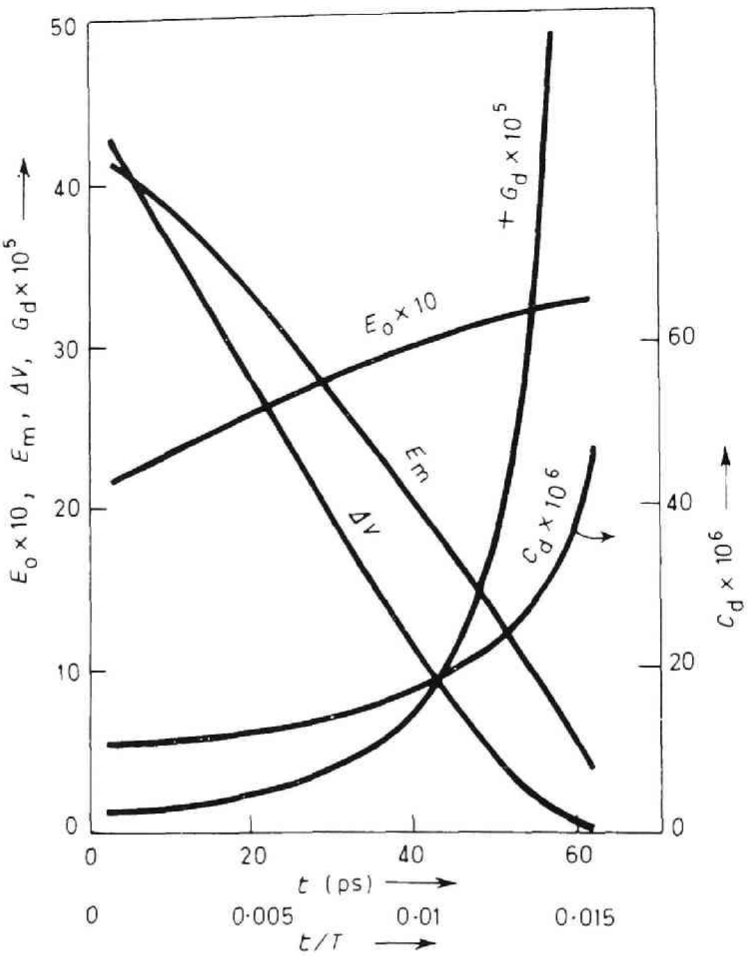

Fig. 6.9 Transient characteristics of domain being extinguished at the anode of diode with $n_0 = 2.0 \times 10^{20}$ m^{-3} and $L = 400$ μm ($n_0 L = 8 \times 10^{12}$ cm^{-2}) and biased at threshold. E_0, E_m, ΔV, G_d and C_d are in the same units as in Fig. 6.5.

the value of 180 ps, since the domain velocity becomes larger as the domain field is decreased (see Fig. 6.4). It is shown in Fig. 6.9 that the capacitance of a domain being extinguished at the anode is increased because the domain width is becoming shorter. The conductance of a domain being extinguished at

the anode is positive and becomes infinite when the domain approaches complete extinction. The variations of the capacitance and the conductance for domain extinction are the inverse of those for domain growth. The sign of the conductance for extinction is opposite to that for growth.

6.7 SUMMARY

Quasi-linear equations have been used to analyze the characteristics of domains in transferred-electron semiconductors. Since the equations have been treated analytically, some physical interpretations have been given to the behavior of high-field domains observed in experiments. The analysis shows that the differential mobility appearing in the relaxation time of the large-signal analysis is not the same as that used in the small-signal analysis. The differential mobility of the large-signal analysis, however, becomes equal to that of the small-signal analysis when the domain reduces to a perturbation. It is shown in the analysis that an equivalent admittance of a domain is represented by a parallel connection of capacitance and conductance which vary with time in the transient state. The time-constant of the admittance is shown to equal the dielectric relaxation time plus a term dependent on the diffusion effect. The shape of a domain with a fractional depletion of carriers in the leading edge is expressed by a symmetrical triangle. The shape of a domain with a complete depletion, however, is expressed by an asymmetrical triangle in which the gradient of the leading edge is determined by the density of the ionized impurity and the shape of the trailing edge is determined by

the diffusion effect. The depletion width is equal to the accumulation width for a domain of relatively small field and potential. The depletion width increases relative to the accumulation width after complete depletion appears in the leading edge. The maximum value of the domain potential in a diode biased at the threshold is derived to be approximately 54 % of the threshold voltage. The displacement current of the diode is shown numerically to be very small in comparison with the conduction current. Thus the total current of the diode is given mainly by the conduction current. The characteristics of a domain calculated from the results of the analysis have been given as numerical examples, which show qualitatively good agreement with the measured values of experiments. It has been pointed out that non-linear and parametric operations of transferred-electron diodes can be interpreted by the use of an expression for admittance of the diode in which the effects of rf circuit voltage on the domain are taken into account.

CHAPTER VII EFFECTS OF MAGNETIC FIELD ON ELECTRON TRANSPORT PROPERTIES IN TRANSFERRED-ELECTRON SEMICONDUTORS

7.1 INTRODUCTION

Current instabilities[1] due to negative differential mobility observed in transferred-electron semiconductor, such as n-type gallium arsenide, at a high electric field have stimulated great interest in the transport properties of this kind of material. A great many investigations, both theoretical and experimental, into the transport properties and the transferred-electron oscillations have been conducted.

The application of a transverse magnetic field to a transferred-electron oscillator has led to various effects such as suppression of the oscillation, enhancement of the coherence of the current fluctuations, a decrease of the apparent threshold, a decrease or increase in output power, and other phenomena.[2] - [5] To understand these effects, a knowledge is required of the transport properties of n-GaAs subject to a transverse magnetic field. The Hall mobility and the galvanomagnetic effect of hot electrons in n-GaAs have been experiemntally investigated applying a high field of a microwave frequency.[6], [7]

The velocity-field characteristic of n-GaAs was obtained by using the Monte Carlo technique in which the value of a peak current with the magnetic field is higher than that without the magnetic field.[8] The high-field galvanomagnetic effects of n-GaAs were also investigated through a compromise approach of the displaced Maxwellian distribution of electron density and

the distribution approximated by the first two terms in its Legendre series expansion.[9] The terms symmetric in momentum are Maxwellian functions at effective carrier temperatures which are determined by the energy balance condition, and the terms asymmetric in momentum are determined as functions of applied field from Boltzmann's transport equation. In this theoretical work, the peak value of a current is low compared with that in the zero magnetic field. Except for a shift of the threshold field to a higher value, the results of magnetic effects in experimental and theoretical works have been rather dissimilar.

The electron transfer and the transport properties of n-GaAs in crossed electric and magnetic fields are described in this chapter, deriving the distribution function through the Conwell and Vassell approach,[10] and measuring the current-field characteristic by the microwave technique.

For simplicity, the distribution functions are derived assuming that the band structure of the lower valley is parabolic. This assumption tends to shift the threshold field to a lower value, since for the parabolic case the electrons are hotter than for the nonparabolic.[10], [12]

7.2 BOLTZMANN'S EQUATIONS FOR A TRANSFERRED-ELECTRON SEMICONDUCTOR

Boltzmann's equations are derived for a transferred-electron semiconductor subject to an electric field E_x applied in the x-direction and a magnetic field B in the z-direction. We first consider the equation for the lower valley. The distri-

bution function is approximated by the first two terms in its Legendre series:

$$f^{(1)}=f_1+k_x g_{\mathfrak{x}\mathfrak{y}}+k_y g_{\mathfrak{y}\mathfrak{y}}, \tag{7.1}$$

where f_1 is the term symmetric in momentum, $g_{\mathfrak{x}\mathfrak{y}}$ and $g_{\mathfrak{y}\mathfrak{y}}$ the terms asymmetric in momentum, and k_x and k_y the x and the y components of the momentum vector k respectively. We assume for simplicity that the band structure of the lower valley is parabolic. The energy ε is thus expressed in terms of the momentum k as $\varepsilon = \hbar^2 k^2/2m_1$ where m_1 is the effective mass in the lower valley, $\hbar = h/2\pi$, and h is Planck's constant.

Boltzmann's equation for a uniform and equilibrium function $f^{(1)}$ is given by

$$\left(\frac{\partial f^{(1)}}{\partial t}\right)_{\boldsymbol{F}}+\left(\frac{\partial f^{(1)}}{\partial t}\right)_c=0. \tag{7.2}$$

The first term expresses the variations of the distribution function resulting from the external forces:

$$\left(\frac{\partial f^{(1)}}{\partial t}\right)_{\boldsymbol{F}}=\frac{q}{\hbar}\left\{\boldsymbol{E}+\frac{1}{\hbar}(\nabla_{\boldsymbol{k}}\varepsilon)\times\boldsymbol{B}\right\}\cdot\nabla_{\boldsymbol{k}} f^{(1)}, \tag{7.3}$$

where q is the electron charge. The substitution of Eq. (7.1) into Eq. (7.3) gives

$$\left(\frac{\partial f^{(1)}}{\partial t}\right)_{\boldsymbol{F}}=\frac{q}{m_1}(\hbar E_x f_1'-B g_{1y})k_x+\frac{q}{m_1}(\hbar E_y f_1'+B g_{1x})k_y+$$

$$\frac{2qE_x}{3\hbar\varepsilon^{\frac{1}{2}}}\frac{\partial}{\partial\varepsilon}(\varepsilon^{\frac{3}{2}}g_{1x})+\frac{2qE_y}{3\hbar\varepsilon^{\frac{1}{2}}}\frac{\partial}{\partial\varepsilon}(\varepsilon^{\frac{3}{2}}g_{1y}), \tag{7.4}$$

where the prime denotes the differentiation with respect to the

energy ε. Here we have replaced the product of the momentum compoenets by its average value; i.e., $\hbar^2 k_x^2/2m_1 = \hbar^2 k_y^2/2m_1 = \varepsilon/3$ and $k_x k_y = 0$ which is an approximation similar to that usually made in the past analysis.[11] The second term in Eq. (7.2) expresses the variations of the distribution function resulting from collisions:

$$\left(\frac{\partial f^{(1)}}{\partial t}\right)_c = \left(\frac{\partial f_1}{\partial t}\right)_c - \frac{1}{\tau^{(1)}}(k_x g_{1x} + k_y g_{1y}), \tag{7.5}$$

where we have assumed the existence of a collision time $\tau^{(1)}$.

The balance, at any momentum, of the variations by the external forces and the collisions implies that terms in different powers of k_x and k_y vanish separately in Eq. (7.2) substituted by Eqs. (7.4) and (7.5).

$$\frac{2q^2(E_x^2+E_y^2)}{3m_1\varepsilon^{\frac{1}{2}}}\frac{\partial}{\partial\varepsilon}\left\{\frac{\varepsilon^{\frac{3}{2}}\tau^{(1)}f_1'}{1+(q\tau^{(1)}B/m_1)^2}\right\} + \left(\frac{\partial f_1}{\partial t}\right)_c = 0, \tag{7.6a}$$

$$g_{1x} = \frac{(q\hbar\tau^{(1)}/m_1)}{1+(q\tau^{(1)}B/m_1)^2}\left\{E_x - \left(\frac{q\tau^{(1)}B}{m_1}\right)E_y\right\}f_1', \tag{7.6b}$$

$$g_{1y} = \frac{(q\hbar\tau^{(1)}/m_1)}{1+(q\tau^{(1)}B/m_1)^2}\left\{\left(\frac{q\tau^{(1)}B}{m_1}\right)E_x + E_y\right\}f_1'. \tag{7.6c}$$

Following the past discussions,[10] the collision time $\tau^{(1)}$ and the collision operator $(\partial f_1/\partial t)_c$ are given by

$$\frac{1}{\tau^{(1)}} = \frac{1}{\tau_{po}} + \frac{1}{\tau_{1\to 2}}, \tag{7.7a}$$

$$\left(\frac{\partial f_1}{\partial t}\right)_c = \left(\frac{\partial f_1}{\partial t}\right)_{po} + \left(\frac{\partial f_1}{\partial t}\right)_{1\rightleftarrows 2}, \tag{7.7b}$$

where the first terms in both equations represent the polar optical scattering and the second terms the intervalley scattering from the lower valley to the upper valleys.

The upper valleys of the conduction band in n-GaAs are along the <100> directions, 0.36 eV above the lower valley. Since the characterisitc features of the many-valley solutions can be neglected, it should be a good approximation to assume the distribution to be the same for each valley with spherical constant energy surfaces.[10] Thus, with the same approach used to obtain the equations for the lower valley, we can derive the equations for the upper valley:

$$\frac{2q^2(E_x^2+E_y^2)}{3m_2(\varepsilon-\varepsilon_0)^{\frac{1}{2}}}\frac{\partial}{\partial\varepsilon}\left\{\frac{(\varepsilon-\varepsilon_0)^{\frac{3}{2}}\tau^{(2)}f_2'}{1+(q\tau^{(2)}B/m_2)^2}\right\}+\left(\frac{\partial f_2}{\partial t}\right)_c=0, \tag{7.8a}$$

$$g_{2x}=\frac{(q\hbar\tau^{(2)}/m_2)}{1+(q\tau^{(2)}B/m_2)^2}\left\{E_x-\left(\frac{q\tau^{(2)}B}{m_2}\right)E_y\right\}f_2', \tag{7.8b}$$

$$g_{2y}=\frac{(q\hbar\tau^{(2)}/m_2)}{1+(q\tau^{(2)}B/m_2)^2}\left\{\left(\frac{q\tau^{(2)}B}{m_2}\right)E_x+E_y\right\}f_2', \tag{7.8c}$$

where the value of ε_0 is 0.36 eV which is the energy difference between the minimums of the upper and the lower valleys. Here the collision time $\tau^{(2)}$ and the collision operator $(\partial f_2/\partial t)_c$ are given by

$$\frac{1}{\tau^{(2)}}=\frac{1}{\tau_a}+\frac{1}{\tau_{po}}+\frac{1}{\tau_{2\to1}}+\frac{1}{\tau_{j\to j'}}, \tag{7.9a}$$

$$\left(\frac{\partial f_2}{\partial t}\right)_c=\left(\frac{\partial f_2}{\partial t}\right)_a+\left(\frac{\partial f_2}{\partial t}\right)_{p0}+\left(\frac{\partial f_2}{\partial t}\right)_{2\rightleftarrows1}+\left(\frac{\partial f_2}{\partial t}\right)_{j\rightleftarrows j'}, \tag{7.9b}$$

where the first terms in both equations represent the acoustic mode scattering and the last terms the equivalent intervalley scatterings in the upper valleys.

7.3 DISTRIBUTION FUNCTIONS

The symmetric terms f_1 and f_2 can be found by integrating Eqs. (7.6a) and (7.8a) which are simultaneous second-order differential equations with variable coefficients. The equations are simultaneous in f_1 and f_2 because they couple through the collision operators, $(\partial f_1/\partial t)_{1\rightleftarrows 2}$ and $(\partial f_2/\partial t)_{1\rightleftarrows 2}$, of the intervalley scattering which are expressed by f_1 and f_2. Once f_1 and f_2 are derived as a function of the energy ε, the asymmetric terms g_{1x}, g_{1y}, g_{2x}, and g_{2y} are obtained from Eqs. (7.6b), (7.6c), (7.8b), and (7.8c) respectively.

The intervalley scattering is insignificant in the energy region $\varepsilon < 0.36$ eV, below the bottom of the upper valley. Thus, for $\varepsilon < 0.36$ eV, Eq. (7.6a) can be solved alone, taking account of only the polar scattering time and operator. To begin the integration of Eq. (7.6a), we must choose the values of $f_1(0)$ and $f_1'(0)$. The value of $f_1(0)$ is determined by normalizing the integration to give the number of electrons. For facilitating the analysis, $f_1(0) = 1$ is chosen at first. An approximation method is used to avoid difficulty in determing the value of $f_1'(0)$. For the energy being much greater than a phonon energy, $\varepsilon \gg 0.036$ eV, Eq. (7.6a) is reduced to a first-order differential equation which may be integrated by using the boundary condition, $f_1(0) = 1$. Thus, the symmetric term f_1 for $\varepsilon <$

0.36 eV can be numerically derived in such a way that f_1 can approach asymptotically for a large energy value. The numerical values of the asymptotic curve for $\varepsilon < 0.36$ eV are taken as a solution for f_1 below the bottom of the upper valley.

For $\varepsilon \geqslant 0.36$ eV, Eqs. (7.6a) and (7.8a) must be integrated simultaneously since the intervalley scattering is dominant in the energy region beyond the bottom of the upper valley. The values of $f_1(0.36)$, $f_1'(0.36)$, $f_2(0.36)$, and $f_2'(0.36)$ must be known. The first two are known from the numerical integration of f_1 for $\varepsilon = 0.36$ eV, but the value of $f_2(0.36)$ and $f_2'(0.36)$ are left unknown. The value of the symmetric terms f_1 and f_2 for $\varepsilon \geqslant 0.36$ eV, however, can be obtained from the approximation method in which Eqs. (7.6a) and (7.8a) are reduced to a first-order equation for $\varepsilon \gg 0.36$ eV, and they are reduced to difference equations valid for a small range of energy for $\varepsilon \geqslant 0.36$ eV. Giving arbitrary values to $f_2(0.36)$ and $f_2'(0.36)$, we determine f_1 and f_2 for $\varepsilon \geqslant 0.36$ eV in such a way that f_2 obtained from the difference equations approaches asymptotically to f_2 obtained from the first-order equation, and the values of f_1 and f_2 remain positive in the range of energy with which we are concerned in the analysis. When these conditions are not satisfied, the difference equations and the first-order equation are again integrated by using $f_2(0.36)$ and $f_2'(0.36)$ with differnt values from the preceeding trials.

The Hall field counteracts the deflection of the electron motion caused by a transverse magnetic field and reduces the effect of a magnetic field on transport properties. To observe the maximum effect of the magnetic field, analysis is made for

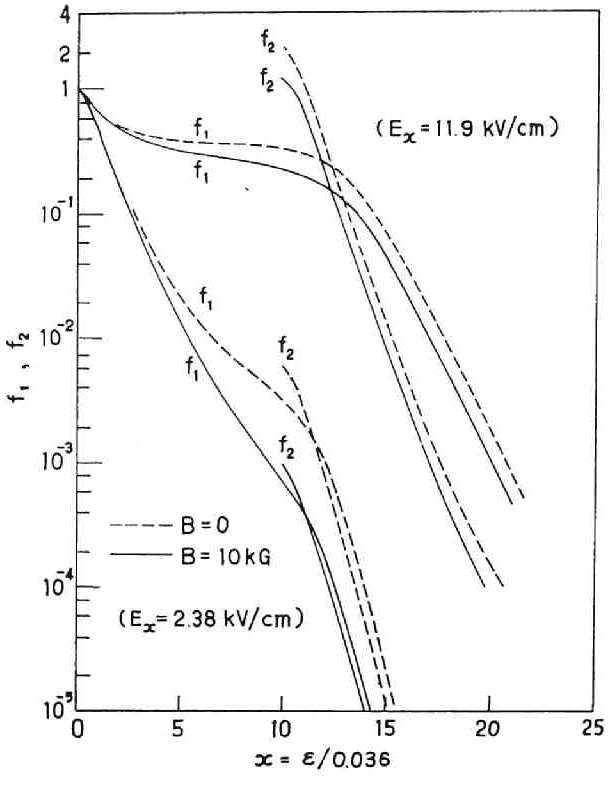

Fig. 7.1 Symmetric terms of distribution functions for electron density in the (0, 0, 0) and <100> valleys with and without magnetic field. (Distributions with the magnetic field 5 kG have been obtained to derive the transport properties, but not shown in this figure for simplicity.)

the Hall field E_y neglected in Eqs. (7.6a) and (7.8a).

It can be seen in those equations that the magnetic field reduces the collision time $\tau^{(1)}$ and $\tau^{(2)}$ respectively to $\tau^{(1)}/\{1 + (q\tau^{(1)}B/m_1)^2\}$ and $\tau^{(2)}/\{1 + (q\tau^{(2)}B/m_2)^2\}$; the larger the collsion time and the less the effective mass, the larger the effect of a magnetic field. To perform the integrations numerically, the values of the physical parameters are referred from

the Conwell and the Vassell paper.[10] The intervalley and the equivalent-intervalley deformation potentials, D_{12} and $D_{jj'}$ are taken as 5×10^8 eV/cm and 1×10^9 eV/cm respectively.

The symmetric terms of the distribution functions are shown in Fig. 7.1 where the hyphenated and the solid lines denote the absence and the presence of a magnetic field 10 kG respectively. The abscissa denotes the energy normalized by the phonon energy $\hbar\omega_1 = 0.036$ eV. The values of f_1 decrease rapidly beyond $x = 10$ where the electron transfer occurs significantly from the lower valley to the upper valleys. The result indicates that the number of electrons in the higher energy region is reduced in the presence of a magnetic field, which can be called the cooling effect of the magnetic field.

The energy is supplied from the electric field to electrons and it is evaluated by $-qE_x v_x \tau$ where v_x is the velocity component along the field and τ the collision time. Although in the absence of the electric field the electrons distribute symmetrically in the velocity space, by the application of an electric field the electrons stream on the average along the opposite direction of the electric field and obtain the energy in a drift motion. However, the elastic scatterings will oppose the streaming tendency and tend to randomize the distribution. Thus, part of the energy in the drift motion turns to the energy in the random motion. Because the electrons are accelerated for the collision time τ which is reduced to $\tau/\{1 + (q\tau B/m)^2\}$ with a magnetic field, the drift velocity is reduced along the electric field; this is known as the magnetoresistance effect. Because of the decrease in the drift velocity and the reduced value of τ in

$-qE_x v_x \tau$, the application of the magnetic field reduces not only the energy in the drift motion but also the energy in the random motion. The latter effect can be called the cooling effect of the magnetic field.

7.4 ELECTRON TRANSFER AND TRANSPORT PROPERTIES

The electron transfer and the transport properties can be obtained once the distributions of the electron density are found. Integrating f_1 from zero to infinity and f_2 from ε_0 to infinity, we obtain the electron concenrations n_1 in the lower valley and n_2 in the upper valley respectively. The total electron concentration n_T is thus given by $(n_1 + n_2)$.

$$n_T = 8\sqrt{2}\pi m_1^{3/2} a (I_1 + I_2)/h^3 , \tag{7.10}$$

where

$$I_1 = \int_0^\infty \gamma^{1/2}(\varepsilon)\gamma'(\varepsilon) f_1(\varepsilon) d\varepsilon , \qquad \gamma^{1/2}(\varepsilon)\gamma'(\varepsilon) \simeq \varepsilon^{1/2} \tag{7.11a}$$

$$I_2 = \left(\frac{m_2^{(N)}}{m_1}\right)^{3/2} \int_{\varepsilon_0}^\infty (\varepsilon - \varepsilon_0)^{1/2} f_2(\varepsilon) d\varepsilon , \tag{7.11b}$$

Here a is the normalization constant of the distribution and $m_2^{(N)}$ the density-of-states mass. The first terms of Eq. (7.10) corresponds to the electron concentration n_1 in the lower valley and the second to the electron concentration n_2 in the upper valleys. Thus we obtain the concentration ratio:

$$r = \frac{n_1}{n_1 + n_2} = \frac{I_1}{I_1 + I_2} . \tag{7.12}$$

The result is shown in Fig. 7.2 where the electron transfer

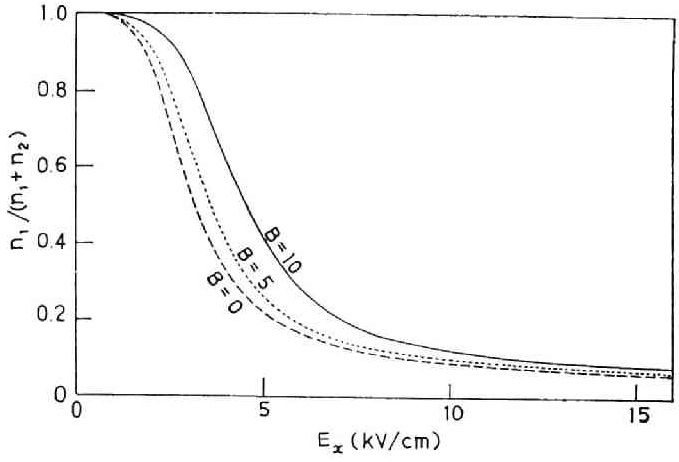

Fig. 7.2 Fraction of electrons in the (0, 0, 0) valley with and without magnetic field.

to the upper valleys occurs less in the presence of a magnetic field than in its absence. The decrease of the transfer can be understood by the cooling effect of the magnetic field on the electron energy.

The drift velocity v_{dx} along the electric field is obtained from the average over the two valleys of current density J_x:

$$J_x = n_T q v_{dx} = \frac{2qn_T(J_1+J_2)}{3h(I_1+I_2)} , \tag{7.13}$$

where

$$J_1 = \int_0^\infty \varepsilon^{3/2}(\varepsilon) g_{1x}(\varepsilon) d\varepsilon , \qquad \gamma^{3/2}(\varepsilon) = \varepsilon^{3/2} \tag{7.14a}$$

$$J_2 = \left(\frac{m_2^{(N)}}{m_1}\right)^{3/2} \frac{m_1}{m_2} \int_{\varepsilon_0}^\infty (\varepsilon-\varepsilon_0)^{3/2} g_{2x}(\varepsilon) d\varepsilon . \tag{7.14b}$$

The drift velocity is expressed as the average drift velocity of the electrons in the lower and the upper valleys:

$$v_{dx} = r v_{dx1} + (1-r) v_{dx2} , \tag{7.15}$$

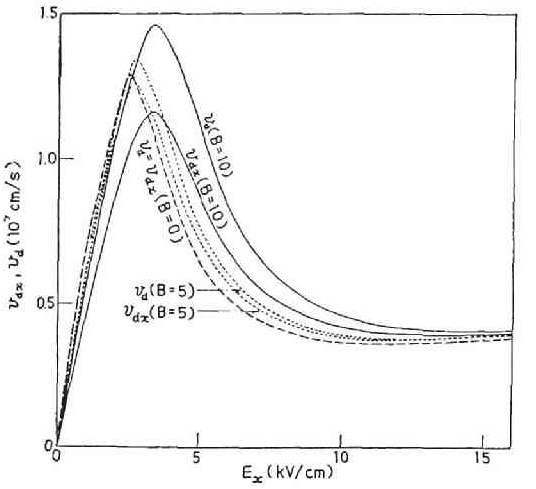

Fig. 7.3 Drift velocity-electric field characteristic with and without magnetic field.

where subscripts 1 and 2 are for the lower and the upper valleys respectively. The total drift velocity $v_d = \sqrt{v_{dx}^2 + v_{dy}^2}$ is obtained from the average over the two valleys of the electron velocities v_{d1} and v_{d2} respectively. The results are shown in Fig. 7.3 where $v_{dx} = rv_{dx1} + (1-r)v_{dx2}$ and $v_d = rv_{d1} + (1-r)v_{d2}$. With the magnetic field, the ratio r increases because of the decrease in the electron transfer to the upper valleys, and the velocitites v_{dx1} and v_{dx2} decrease because of the magnetoresistance effect on the electrons in each valley. As can be seen in Fig. 7.3, the drift velocity v_{dx} is reduced in the low-field region where the magnetoresistance effect predominates. The threshold field shifts to a higher field because the magnetic cooling effect requires more field for the electron transfer to realize a negative differential mobility. The drift

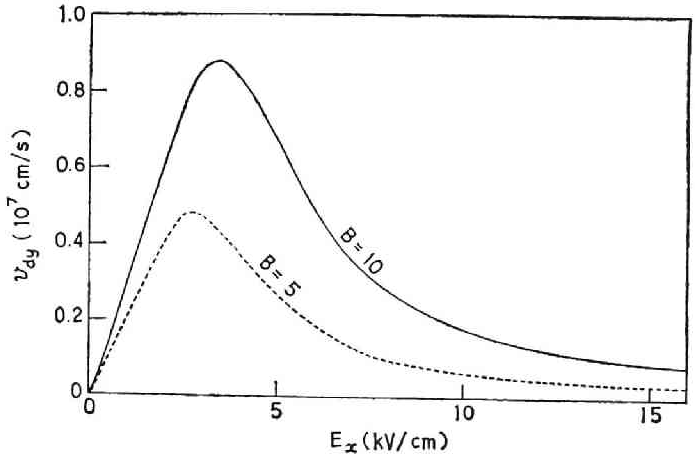

Fig. 7.4 Variations of drift velocity v_{dy} with applied electric field E_x.

velocity v_{dx} increases in a high-field region where more electrons are left in a lower valley with a high mobility. Because the magnetic cooling effect predominates over the magnetoresistance effect, the negative effect of the magnetoresistance appears in n-GaAs where there exist two species of electrons with different mobilities.

We can see in the presence of a magnetic field that the peak value increases in total drift velocity in which a magnetic cooling effect predominates over the magnetoresistance effect. With certain scattering times and operators, we could expect such an electron transfer that a magnetic cooling effect is strong enough for the peak value of the drift velocity v_{dx} to increase.

The drift velocity v_{dy} perpendicular to the electric field is given in Fig. 7.4 where the differential mobility $(\partial v_{dy}/\partial E_x)$ is negative in a high-field region. The negative value can be understood because the galvanomagnetic effect is proportional

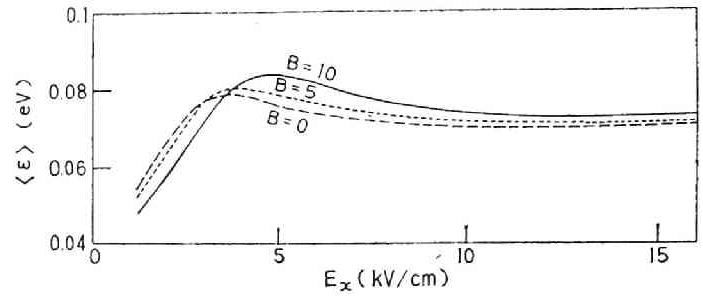

Fig. 7.5 Energy in the random motion with and without magnetic field.

to the drift velocity v_{dx} which shows a negative differential mobility in n-GaAs. Thus, in the presence of the magnetic field, a fraction of an oscillation power can be obtained along the direction perpendicular to the applied electric field E_x. It was found in a recent work[13] that the carrier waves are skewed in the presence of a magnetic field. The flow of a fraction of power in a sample is inverted when a magnetic field is directed to a negative z - direction. The energy in the random motion, $<\varepsilon>=r<\varepsilon_1>+(1-r)<\varepsilon_2>$, and the diffusion coefficient, $D=rD_1+(1-r)D_2$, are given in Figs. 7.5 and 7.6 respectively. We can see in the presence of a magnetic field that both $<\varepsilon>$ and D decrease in a low-field region where the number of electrons with higher energy decrease due to the magnetic cooling effect, and that they increase in a high-field region where more electrons remain in the lower valley due to the magnetic cooling effect. The transport properties are mainly determined by the electrons in the lower valley although in the high-field region the most electrons are in the upper valley.

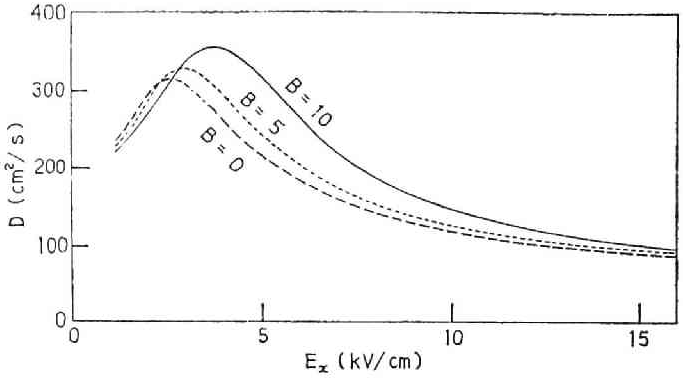

Fig. 7.6 Diffusion coefficient with and without magnetic field.

7.5 MEASUREMENT OF CURRENT-FIELD CHARACTERISTIC

A microwave electric field is used to measure the current-field characteristic of n-GaAs. A uniform distribution of the applied field can be expected in a sample when the period of the microwave frequency is too short for the field distribution to be distorted due to the negative differential mobility. When the capacitance of the Schottky barrier formed by the contact of the waveguide wall and the sample of n-GaAs becomes a small enough component of the impedance in a microwave frequency to shorten the contact electrically, Ohmic electrodes of the sample are not required.

The schematic diagram of the experiment is shown in Fig. 7.7. The microwave field is generated in 9 GHz by the M167 type magnetron which is driven by the high voltage of a pulse with a width of 1μ second. The repetition rate of the pulse is chosen as 10 Hz to avoid heating the sample. The sample, about 5.0 x 2.6 x

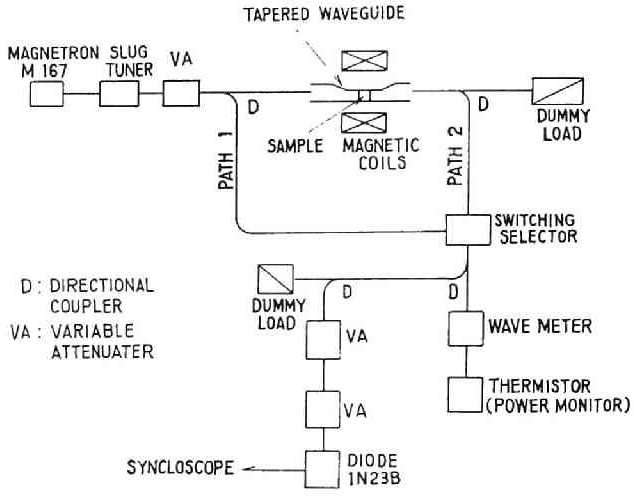

Fig. 7.7 Schematic diagram for the measurement of the current-field chracteristic by high-power microwave.

0.32 mm in size, is mounted inside the waveguide which is tapered to 5 mm in height. The microwave field is applied along the length of the sample and the magnetic field is applied perpendicular to the broad face of the sample.

There has been derived theoretically the restriction, $\rho_0 f \geqslant 35$, on the product of the low-field resistivity ρ_0 Ω-cm and the microwave frequency f GHz to prevent the field from being distorted in n-GaAs.[17] Field distortion may occur in a sample of low resistivity, but the accuracy of the measurement may suffer in a sample of high resistivity because the absorption of microwave power is small and it is hardly detected in the measurement. The sample of 12 Ω- cm was used in the experiment, and the electron concentration is 9.8×10^{13} cm^{-3}.

The current density is expressed in terms of the applied field E:

$$J(E)=\sigma_0 E(1+\zeta E^2+\xi E^4)\,, \tag{7.16}$$

where σ_0 is the low-field conductivity and ζ and ξ are the coefficients to be determined by the experiment. When the microwave field is given by $E=E_1\cos\omega t$, the absorbed power of the sample is evaluated by

$$\begin{aligned} P_{abs}&=\frac{V}{2\pi}\int_0^{2\pi} J(E_1\cos\omega t)E_1\cos\omega t\,\mathrm{d}(\omega t)\\ &=\frac{V\sigma_0}{2}\left(1+\frac{3}{4}\zeta E_1^2+\frac{5}{8}\xi E_1^4\right). \end{aligned} \tag{7.17}$$

The absorbed power is measured from the difference between powers transmitted to the detector through path 1 and path 2. We determine the coefficients ζ and ξ by the least square method, using the value of the absorbed power P_{abs} and the microwave peak field E_1[18] which were taken in the measurement. The current-field characteristic of n-Ge with 8 Ω - cm was measured to confirm the validity of the measurement of P_{abs} and E_1. The result is closely similar to the characteristic which was measured by a different procedure and has been widely accepted.[19]

The current-field characteristic of n-GaAs is shown in Fig. 7.8. It can be seen in the figure that the application of the magnetic field decreases the peak value of the current and shifts the threshold to a higher field, and in a high-field region increases the value of the current, *i.e.*, a negative magnetoresistance effect. The results agree qualitatively with the theoretical ones described in the preceding section. The character-

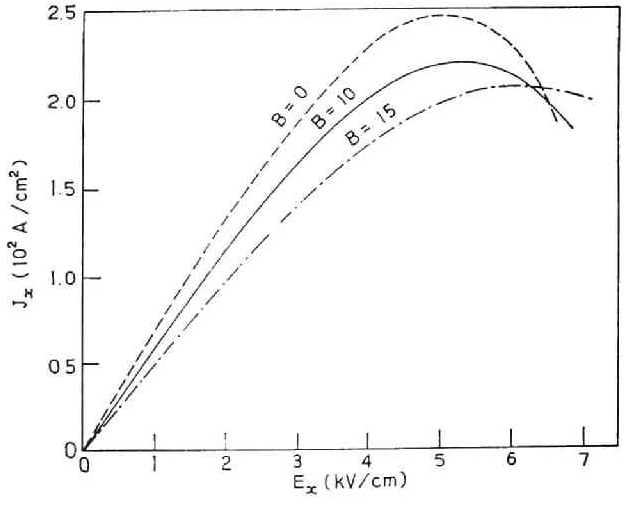

Fig. 7.8 Measured current-electric field characterisitc with and without magnetic field.

istic in the absence of the magnetic field shows in the experiment that the threshold appears near 5 kV/cm. This can be attributed to the imperfection in the contact of the sample to the waveguide wall. The experimental results may not be referred for quantitative discussion. The decisive conclusion of the effect on the negative differential mobility was left to a further study since improvement in the experiment is required to prevent the electrical discharge along the sample surface.

7.6 SUMMARY

The effects of the magnetic field on the electron transfer and transport properties have been investigated theoretically and experimentally. The magnetic field decreases not only the drift velocity along the applied electric field but also the

energy in the random motion of the electrons in a single valley; the former is known as the magnetoresistance effect and the latter can be termed the cooling effect of the magnetic field. Due to the cooling effect the rate of the electron transfer from the lower valley to the upper valley is reduced in a transferred-electron semiconductor.

The effects of the magnetic field on the velocity-field characteristic can be summarized as follows: (1) the drift velocity along the electric field decreases in a low-field region where the magnetoresistance effect predominates, whereas it increases (*i.e.*, a negative magnetoresistance effect) in a high-field region, where the magnetic cooling effect predominates; (2) the threshold field shifts to a higher field, because the magnetic cooling effect requires a higher intensity of the field for the electron trnasfer to realize a negative differential mobility; (3) the peak value of the total drift velocity increases, *i.e.*, a negative magnetoresistance effect, because more electrons are left in a lower valley with a high mobility; (4) the differential mobility ($\partial v_{dy}/\partial E_x$) can be negative; and (5) the energy in the random motion and the diffusion coefficient decrease in a low-field region and increase in a high-field region.

The experiment to measure the current-field characteristic by the microwave technique shows qualitative agreements with the characteristic obtained by the theory. The experiment on a negative differential mobility has been left to a further study. It has to be noticed that the theoretical results have been obtained to see the maximum effect of the magnetic field neglecting the Hall field. It must be taken into account for each practi-

cal case in a further study. It may prove possible for the peak value of the drift velocity to increase when the magnetic cooling effect predominates over the magnetoresistance effect below the threshold field.

CHAPTER VIII WAVE INSTABILITIES IN BULK SEMICONDUCTORS WITH FIELD-DEPENDNET DRIFT VELOCITY AND CARRIER TEMPERATURE

8.1 INTRODUCTION

The Boltzmann equation and the Poisson equation are often used to analyze wave instabilities in semiconductors. A set of transport equations, which describe macroscopically observable phenomena, can be derived from the Boltzmann equation. When we write these equations in the order of increasing powers of the carrier velocity, they are called the continuity equation, the momentum equation, the temperature equation (customarily called the energy equation), and so on.

The analysis in this paper was stimulated by observed wave instabilities in microwave bulk semiconductor devices such as avalanche diodes[1] and transferred-electron diodes.[2] An avalanche diode (transferred-electron diode) is considered to be a diode in which wave instability associated with the continuity equation (momentum equation) is utilized to generate rf power since the instability is caused by changes in carrier density (changes in carrier momentum). Thus we may investigate the existence of wave instabilities associated with the energy equation. Such wave instabilties, caused by changes in carrier temperature, are of interest as a new class of instabilites capable of being utilized for the generation of rf power.

We assume that the semiconductor is extrinsic, in which one species of carrier exists, and that the mobility and the energy

relaxation time depend non-linearly on the carrier temperature. The avalanche and the recombination of carriers are neglected in order to confine the analysis to wave instabilites caused by the field dependencies of the drift velocity and the carrier temperature. The results are compared with the small-signal instability of the transferred-electron diode[2] and the diffusion instability[3] in semiconductors. Although the analysis is presented with reference to semiconductors, it is equally valid for a collision-dominated, weakly ionized gas plasma.

8.2 LIMITATION ON INSTABILITIES

The kinetic energy of carriers is given by the sum of the drift energy and random energy. The drift energy, which is expressed by $m^*v^2/2$, results from the drift motion of carriers. The random energy, which is expressed by $3kT/2$, results from the random motion of carriers. Here m^* is the effective mass, v is the drift velocity, k is the Boltzmann constant, and T is the carrier temperature. An external field supplies carriers with drift energy $q\tau_{p0}E_0v_0/2$ and random energy $2q\tau_{e0}E_0v_0/3$, where the momentum relaxation time τ_{p0} is in most cases in semiconductors much less than the energy relaxation time τ_{e0}. Here the subscript 0 represents the value at dc state. The kinetic energy of carriers, thus, can be approximated by the random energy.

The tmeperature of the host lattice has been treated as constant in many earlier analyses. The lattice temperature must increase since the kinetic energy supplied to carriers by an

external field is transferred to the host lattice through collisions. On considerations of energy conservation, we have to take not only the energy of carriers but also the energy of the host lattice. The total energy can be written as

$$\mathcal{E}_{t0}=(3k/2)[(n_0T_0+N_0T_{L0})/(n_0+N_0)], \tag{8.1}$$

where n_0 denotes the carrier density, N_0 the density of the lattice, and T_{L0} the lattice temperature. When no external field is applied to the carriers at thermal equilibrium, the carrier temperature equals the temperature of the host lattice. The $\varepsilon_{t0}=3kT_{L00}/2$, where T_{L00} is the lattice temperature at zero external field. From the thermodynamic considerations we may require that positive dependency of the energy on the field, $\partial\varepsilon_{t0}/\partial E_0>0$, must hold. The wave instabilities caused by $\partial T_0/\partial E_0<0$ must be examined subject to the condition $\partial\varepsilon_{t0}/\partial E_0>0$. From Eq. (8.1) we obtain the condition for $\partial\varepsilon_{t0}/\partial E_0$ to be positive:

$$T_1>-(N_0T_{L0}/n_0T_0)T_{L1}, \tag{8.2}$$

where T_1 represents the field dependency of the carrier temperature, given by $(E_0/T_0)\partial T_0/\partial E_0$, and T_{L1} represents the field dependency of the lattice temperature, given by $(E_0/T_{L0})\partial T_{L0}/\partial E_0$. The limitation given by Eq. (8.2) should be taken into account in the study of the wave instabilities caused by negative dependency of the carrier temperature on the field. When we consider the potential energy of carriers, the limitation given by Eq. (8.2) is modified.

8.3 DISPERSION RELATION

The assumptions which we use in the analysis are listed as follows:

(1) Carriers have positive charge and the results of the analysis may be applied to an n - type semiconductor by changing the sign of the charge;

(2) quasi-one-dimensional analysis is used;

(3) dc quantities are uniform in space and small-signal theory is used;

(4) phenomena are adiabatic, i.e., heat flow is zero; and

(5) generation and recombination of carriers are zero.

The transport equations can be derived from the Boltzmann equation by using phenomenological expressions of the collision terms[4], [5]: $-nm^*v/\tau_p$ in the momentum equation and $-(3/2)\cdot kn(T-T_L)/\tau_e$ in the energy equation. Here n is the carrier density and τ_e is the energy relaxation time. The continuity equation is

$$(\partial n/\partial t)+(\partial/\partial \chi)(nv)=0. \tag{8.3}$$

The momentum equation is

$$\frac{\partial v}{\partial t}+v\frac{\partial v}{\partial \chi}+\frac{k}{mn}\cdot\frac{\partial}{\partial \chi}(nT)-\frac{q}{m}E=-\frac{v}{\tau_p}. \tag{8.4}$$

The energy equation is

$$\frac{\partial T}{\partial t}+v\frac{\partial T}{\partial \chi}+\frac{2}{3}T\frac{\partial v}{\partial \chi}=-\frac{T-T_L}{\tau_e}+\frac{2mv^2}{3k\tau_p}. \tag{8.5}$$

To derive the dispersion relation, Poisson's equation is used:

$$\partial E/\partial \chi = (q/\epsilon)(n - n_0), \tag{8.6}$$

where ϵ is the dielectric constant of the semiconductor and n_0 is the density of ionized impurity, which is equal to the carrier density at dc state.

In the microwave frequency region, in which wave instabilities will be examined, we may assume in semiconductors that

$$\omega\tau_p \ll 1 \quad \text{and} \quad \beta v_0 \tau_p \ll 1, \tag{8.7}$$

where ω is the angular frequency and β is the phase constant. Thus the analysis is valid when the variations of wave disturbances are slow in time and space as compared with the microscopic variations due to collisions with the lattice. Using this assumption we can write Eq. (8.4) as

$$v = \mu E - (k\mu/qn) \cdot (\partial/\partial \chi)(nT). \tag{8.8}$$

In small-signal analysis, quantities are divided into dc and ac components. We denote a dc component by the subscript 0, such as E_0, and an ac component by δ, such as δE. The mobility μ and the effective mass m^* are considered in this analysis to be functions of the carrier temperature T. First we obtain dc equations:

$$v_0 = \mu_0 E_0 \tag{8.9}$$

$$T_0 = T_{L0} + (2/3k) q\tau_{e0} E_0 v_0 \qquad \text{(Ref. 6)}. \tag{8.10}$$

Second, neglecting the product of ac terms, we obtain ac equations:

$$\frac{\partial}{\partial\chi}\delta v=-j\frac{\omega}{\omega_c}\cdot\frac{\partial}{\partial\chi}(\mu_0\delta E)-\frac{v_0}{\omega_c}\cdot\frac{\partial^2}{\partial\chi^2}(\mu_0\delta E), \tag{8.11}$$

$$\delta v=\mu_0\delta E+\frac{kE_0}{q}\cdot\frac{\partial\mu_0}{\partial T_0}\delta T-\frac{k\mu_0}{q}\cdot\frac{\partial}{\partial\chi}\delta T-\frac{k\mu_0T_0}{q\omega_c}\cdot\frac{\partial^2}{\partial\chi^2}(\mu_0\delta E) \tag{8.12}$$

$$\begin{aligned}(1+j\omega\tau_{e0})\delta T=&\frac{4q}{3k}\tau_{e0}E_0\delta v+j\tfrac{2}{3}\tau_{e0}T_0\frac{\omega}{\omega_c}\cdot\frac{\partial}{\partial\chi}(\mu_0\delta E)+\tfrac{2}{3}\cdot\frac{\tau_{e0}v_0T_0}{\omega_c}\cdot\frac{\partial^2}{\partial\chi^2}(\mu_0\delta E)\\&+\frac{2v_0^2\tau_{e0}}{3k\tau_{p0}}\cdot\frac{\partial m_0^*}{\partial T_0}\delta T+\frac{2m_0^*v_0^2}{3k}\cdot\frac{\partial}{\partial T_0}\left(\frac{\tau_{e0}}{\tau_{p0}}\right)\delta T-\tau_{e0}v_0\frac{\partial}{\partial\chi}\delta T+\frac{\partial T_{L0}}{\partial T_0}\delta T,\end{aligned} \tag{8.13}$$

where $\omega_c=\mu_0n_0q/\epsilon$ is the inverse of the dielectric relaxation time. Here we have used

$$\mu=\mu_0+(\partial\mu_0/\partial T_0)\delta T$$

$$m^*=m_0^*+(\partial m_0^*/\partial T_0)\delta T. \tag{8.14}$$

The differentiations $\partial\mu_0/\partial T_0$ and $\partial m_0^*/\partial T_0$ can be written as $(\partial\mu_0/\partial E_0)(\partial E_0/\partial T_0)$ and $(\partial m_0^*/\partial E_0)(\partial E_0/\partial T_0)$ since dc quantities are a function of the electric field E_0, as can be seen in dc equations (8.9) and (8.10). To investigate the existence of wave instability, we use the criterion that the condition for wave instability is obtained by requiring the imaginary part of ω to be negative when the propagation constant Γ is replaced by pure imaginary β.[7] Applying the variation $\exp j(\omega t-\beta x)$ to Eqs. (8.11)-(8.13), we derive the dispersion relation:

$$\begin{aligned}&j\frac{5T_1}{4\omega_d^2}(\beta v_0)^3-(2\omega_d)^{-1}\left(1+v_1-\tfrac{7}{2}T_1+j\frac{5\omega}{2\omega_d}T_1\right)(\beta v_0)^2\\&\quad+j\left(1+\frac{3\omega_c}{4\omega_d}T_1+j\frac{5\omega}{2\omega_d}T_1+j\frac{\omega}{2\omega_d}v_1-j\frac{\omega}{2\omega_d}\right)(\beta v_0)\end{aligned}$$

$$-j\omega\left(1+\frac{3\omega_c}{4\omega_d}T_1+j\frac{3\omega}{4\omega_d}T_1-j\frac{\omega_c}{\omega}v_1\right)=0, \qquad (8.15)$$

where v_1 represents the field dependency of the carrier velocity given by $(E_0/v_0)(\partial v_0/\partial E_0)$ and ω_d represents the diffusion effect given by $qv_0^2/k\mu_0 T_0$. The first term in Eq. (8.15) results from nonisothermal phenomena. The second term represents the diffusion effect and the third term represents the propagation of the wave disturbances. The last term expresses that the wave disturbance varies with angular frequency ω affected by $3\omega_c T_1/4\omega_d$, and is attenuated in a semiconductor with diffusion $k\mu_0 T_0/q$ $(1/\omega_d = k\mu_0 T_0/qv_0^2)$ affected by T_1 and with conductivity σ_0 $(\omega_c = \sigma_0/\epsilon)$ affected by v_1.

8.4 WAVE INSTABILITIES

We study here the existence of wave instabilities in semiconductors in which the drift velocity and the carrier temperature depend on the strength of an applied field. From the dispersion relation an imaginary part of ω can be derived as

$$\omega_i=(2\omega_d/3T_1)\{(1+CT_1)\pm(1/\sqrt{2})[(A^2+B^2)^{1/2}-A]^{1/2}\}, \qquad (8.16)$$

where

$$A=(\omega_0/2\omega_d)^2(1-v_1-2T_1)^2+3[(\omega_c/\omega_d)+(\omega_0^2/\omega_d^2)]v_1T_1-(1+CT_1)$$

$$B=(\omega_0/\omega_d)(1-v_1-2T_1)(1+CT_1)$$

$$C=(3\omega_c/4\omega_d)+(5\omega_0^2/4\omega_d^2).$$

Here we have used $\omega_0 \equiv \beta v_0$. By using the criterion, we derive the conditions for wave disturbances to be unstable. The conditions are shown in Fig. 1 and listed as follows (see Appendix):

$$\begin{aligned} &\text{I} \quad v_1<0 \quad \text{and} \quad T_1>0 \\ &\text{II} \quad v_1<0 \quad \text{and} \quad -[(3\omega_c/4\omega_d)+(5\omega_0^2/4\omega_d^2)]^{-1}<T_1<0 \\ &\text{III} \quad v_1>0 \quad \text{and} \quad T_1<0. \end{aligned} \tag{8.17}$$

Taking into account the limitation on instabilities derived in Section 8.2, we can consider two cases: the case $N_0T_{L0}T_{L1}/n_0T_0> 1/[(3\omega_c/4\omega_d)+(5\omega_0^2/4\omega_d^2)]$ which is shown in Fig. 1(a) and the case $N_0T_{L0}T_{L1}/n_0T_0< 1/[(3\omega_c/4\omega_d)+(5\omega_0^2/4\omega_d^2)]$ which is shown in Fig. 1(b). The wave instability in the region denoted by U in Fig. 1 cannot occur because positive dependency of the energy on the field is not satisfied there, i.e., the total energy decreases with the application of an external field.

The wave disturbances are unstable when $T_1 = 0$ and $v_1 < 0$, but not when $T_1 = 0$ and $v_1 \geqslant 0$. The wave instability in region I is caused by the transferred-electron effect, for which the field dependency of the carrier temperature is not required to be negative. The instabilities in regions II and III are the ones associated with the energy equation. In particular, the wave instability in region III is caused only by a negative T_1. Diffusion instability in which an effective diffusion coefficient is negative has been proposed for two species of carriers, electrons and holes.[3] The regions obtained by substracting the region of diffusion instability for one species of carrier from regions II and III may be considered to be the regions of insta-

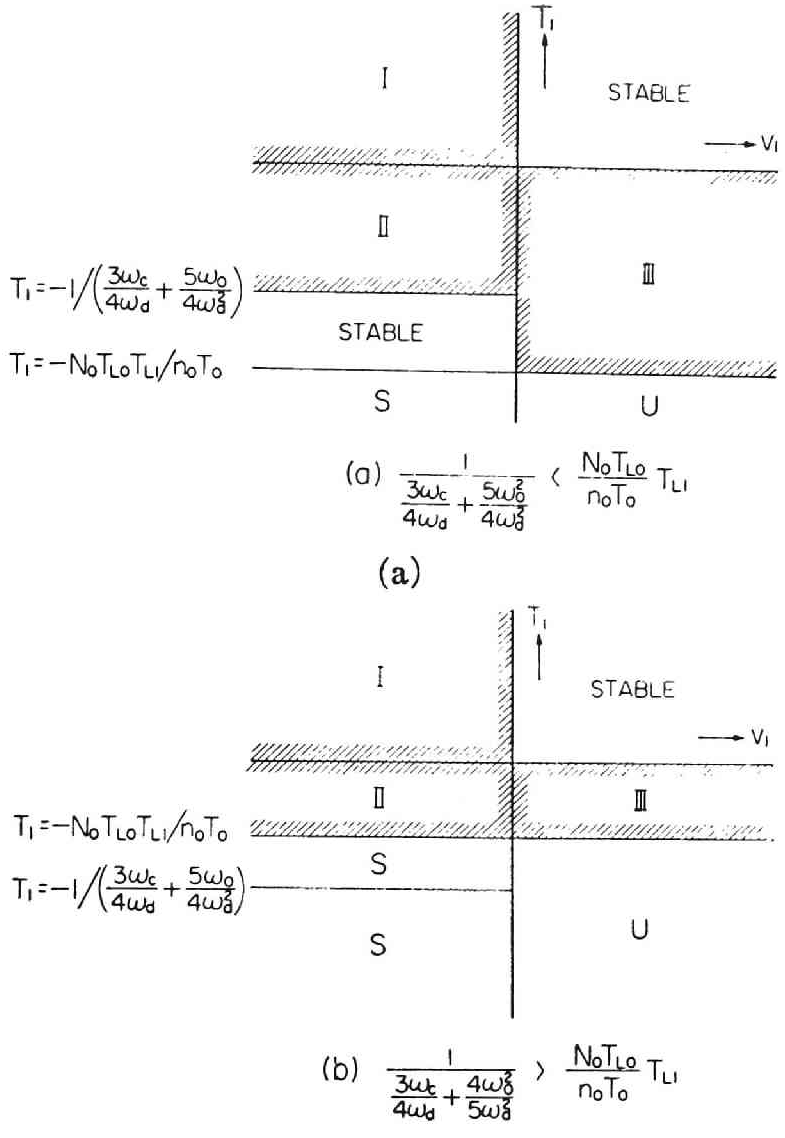

Fig. 8.1 Wave disturbances are unstable in the hatched regions. The notations S and U denote stable and unstable regions, respectively, where positive dependency of the energy on the field is not satisfied.

bility derived in this analysis.

From the diffusion coefficient D_0 defined by $k\mu_0 T_0/q$, we

obtain

$$D_1 = v_1 + T_1 - 1, \tag{8.18}$$

where $D_1 = (E_0/D_0)(\partial D_0/\partial E_0)$ is the field dependency of the diffusion effect. By using Eq. (8.18), we can show unstable regions in the $v_1 - D_1$ diagram as in Fig. 8.2, where the regions denoted by the Roman numerals correspond to those in Fig. 8.1. It can be seen in Fig. 8.2 that we may expect wave instabilities for positive v_1 and D_1 as long as T_1 is negative.

We now study the existence of wave instabilities in a field-independent case in which the mobility and the energy relaxation time do not depend on the strength of an applied field. We assume further that the temperature of the host lattice is constant. From Eqs. (8.9) and (8.10) we obtain

$$v_1 = 1 \quad \text{and} \quad T_1 = 2(T_0 - T_{L0})/T_0 \equiv 2\Delta. \tag{8.19}$$

Applying Eq. (8.19) to Eq. (8.15) we may write the dispersion relation as

$$j\frac{5\Delta}{2\omega_d^2}\omega_0^3 - (\omega_d)^{-1}\left(1 - \tfrac{7}{2}\Delta + j\frac{5\omega}{2\omega_d}\Delta\right)\omega_0^2$$

$$+ j\left(1 + \frac{3\omega_c}{2\omega_d}\Delta + j\frac{5\omega}{\omega_d}\Delta\right)\omega_0$$

$$- j\omega\left(1 + \frac{3\omega_c}{2\omega_d}\Delta + j\frac{3\omega}{2\omega_d}\Delta - j\frac{\omega_c}{\omega}\right) = 0. \tag{8.20}$$

When the carrier temperature T_0 increases over $7T_{L0}/5$, we have a negative real part of the diffusion term, for which an unphysical process in instability has been pointed out.[8] The in-

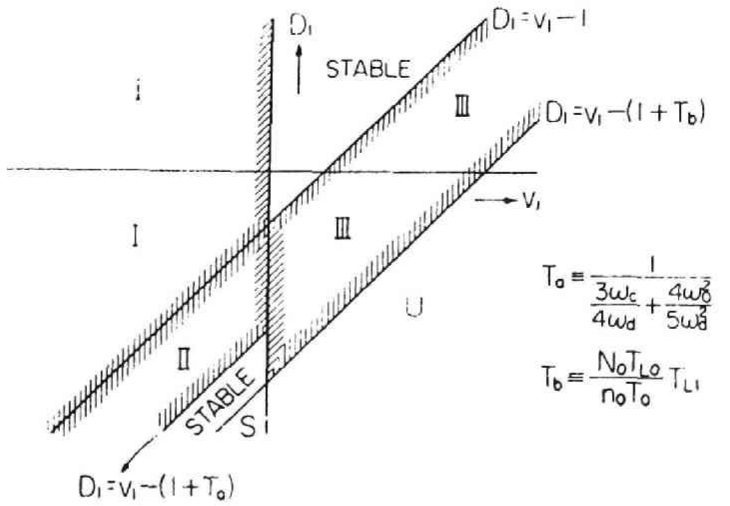

(a) $T_a < T_b$

(a)

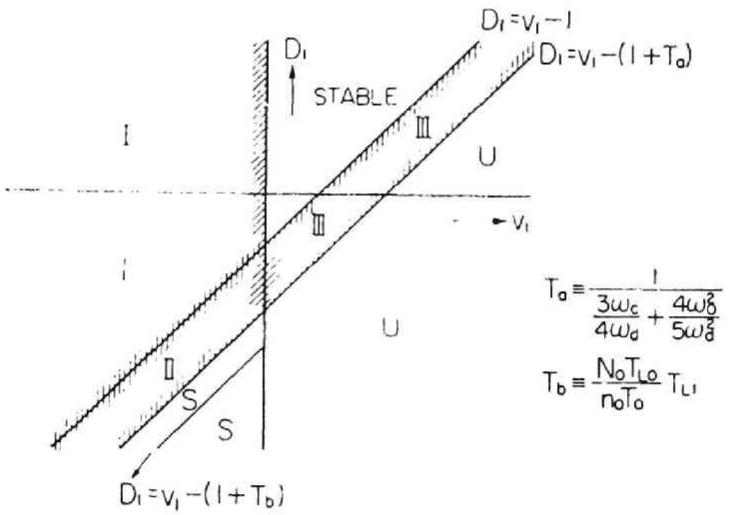

(b) $T_a > T_b$

(b)

Fig. 8.2 Wave disturbances are unstable in the hatched regions. The regions denoted by the Roman numerals correspond to those in Fig. 8.1.

vestigation by the criterion gives the condition for instability,

$$(\omega_0/\omega_d)[(\omega_c/\omega_0)+(\omega_0/\omega_d)]\Delta<0 \tag{8.21}$$

which cannot be satisfied by $T_0 \geq 7T_{L0}/5$. Thus we may not expect instability for a negative real part of the diffusion term in the dispersion relation.

8.5 COMPARISON WITH DIFFUSION INSTABILITY

We have analyzed wave instabilities of one species of carrier, electrons or holes, caused by the field dependency of the drift velocity v_1 and the carrier temperature T_1. The results obtained in this chapter will be compared with diffusion instability, which has been discussed by D. W. Ross,[3] and K. Blötekjaer and P. Weissglas.[3] Diffusion instability is caused when the effective diffusion coefficient D_{eff} is negative. The coefficient D_{eff} has been defined by replacing the temperature gradient by the denisty gradient as

$$\frac{D_{eff}}{n_0}\cdot\frac{\partial}{\partial\chi}\delta n \equiv \frac{k\mu_0}{q}\cdot\frac{\partial}{\partial\chi}\delta T+\frac{k\mu_0 T_0}{qn_0}\cdot\frac{\partial}{\partial\chi}\delta n. \tag{8.22}$$

From Eqs. (8.11) - (8.13) the effective diffusion coefficient is derived as

$$\frac{qD_{eff}}{k\mu_0 T_0}=1+\frac{[(v_{ph}/v_0)-1]+j(2\omega\tau_0/7\omega_d v_{ph})[(v_{ph}/v_0)-1]-j(\omega_c v_{ph}/\omega v_0)}{v_1-(3/7)+j(3\omega/7\omega_d)T_1}T_1, \tag{8.23}$$

where we have used the phase velocity v_{ph} given by ω/β. For simplicity we assume $\omega_c/\omega_d \cong 0$ for which we obtain the real part of the effective diffusion coefficient.

$$\mathrm{Re}\left(\frac{qD_{eff}}{k\mu_0 T_0}\right)=1+\frac{T_1}{v_1-(3/7)}\left(\frac{v_{ph}}{v_0}-1\right). \tag{8.24}$$

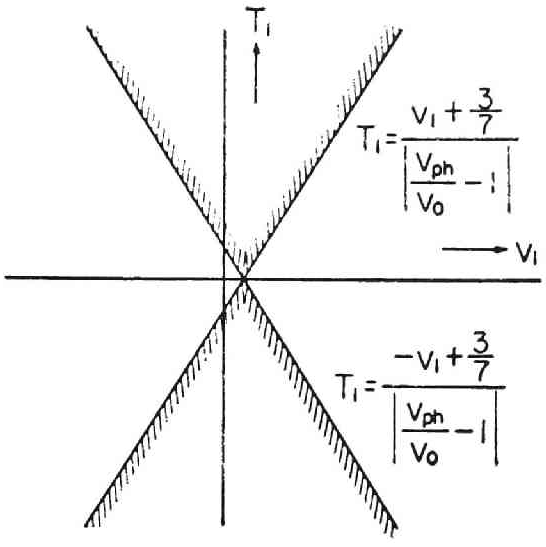

Fig. 8.3 The effective diffusion coefficient is negative inside the hatched regions.

When two species of mobile carriers exist in a semiconductor, the phase velocity v_{ph} of either one of the carriers is slower than the dc velocity. Two species of mobile carriers were taken in the analysis to realize negative $\mathrm{Re}(qD_{eff}/k\mu_0 T_0)$ when the field dependencies of the drift velocity and the carrier temperature are not considered.[3] On the other hand, when the field dependencies are considered, wave instabilities are expected in an extrinsic semiconductor where only one species of carrier exists.

The hatched region in Fig. 8.3 shows the region where $\mathrm{Re}(qD_{eff}/k\mu_0 T_0)$ is negative. The comparison of the negative region of $\mathrm{Re}(qD_{eff}/k\mu_0 T_0)$ with unstable region in Fig. 8.1 indicates that wave disturbances are not always unstable in the case of one species of carrier even if $\mathrm{Re}(qD_{eff}/k\mu_0 T_0)$ is negative.

8.6 SUMMARY

The wave instabilities in avalanche and transferred-electron effect diodes are associated with the continuity and the momentum

equations, respectively. The analysis in this chapter has derived the wave instabilities caused by $v_1 > 0$ and $T_1 < 0$, and $v_1 < 0$ and $T_1 < 0$ as shown in Fig. 8.1. These instabilties are associated with energy equation. The results obtained in this analysis are valid when the drift energy of the carrier is small enough to neglect relative to the random energy . This condition can be satisfied in many cases of semiconductors although the random energy may not reduce without limitation by negative dependence on an external field. We emphasize that the thermodynamic considerations must be taken when negative dependencies of the drift velocity and the carrier temperature are considered. We can expect diffusion instability in an extrinsic semiconductor when the field dependencies are considerd. It must be realized, however, that a negative value of the effective diffusion coefficient does not always lead to wave instability in an extrinsic semiconductor, as can be seen by comparing Fig. 8.3 with Fig. 8.1.

Further investigations open to practical materials in which the wave instabilty is observed associating with the energy equation.[9] The analysis in this chapter is equally valid for a collision-dominated, weakly ionized gas plasma although it has presented with reference to semiconductors.

CHAPTER IX CONCLUSIONS AND SUGGESTIONS FOR FURTHER STUDY

Electronic and microwave properties of transferred-electron semiconductors have been studied and described in this thesis. The results and conclusions obtained in this study can be summarized in the followings.

(1) The condition for differential negative resistance has been obtained in the transferred-electron semiconductors. With this condition, the confusion has been resolved to the two operational modes in the transferred-electron semiconductors: the mode based on the differential negative resistance and the mode based on the current instability.

(2) The conditions for space-charge-wave growth and differential negative resistance have been derived with taking account of the energy transport effect. They can be considered to give more accurate quantitative results as compared with those derived precedently.

(3) It has been shown in a simple analysis that the power-impedance product of the transit-time oscillation in transferred-electron diodes is proportional to the square of the product of the difference between the applied and the sustaining electric fields and the drift velocity, and inversely proportional to the square of the frequency. The result predicts the maximum power output available from the transit-time oscillation of the transferred-electron diodes. The formula for the maximum efficiency in the transit-time oscillation has also been derived.

(4) Self-pumped parametric effects have been described considering the admittance variations of a domain which occur not when the domain grows near the cathode and is quenched at the anode, but when the bias voltage is varied by an rf output voltage. It has been shown that a parametric change in admittance appears in a diode self-pumped by a voltage with a fundamental frequency and that additional admittance appears in a diode self-pumed by a voltage with a harmonic frequency. This study gives the theoretical basis to the self-pumped operation and the increase in the output power with a harmonic frequency in the transferred-electron diodes.

(5) Transient behavior and characteristics of the high-field domain in the transferred-electron diodes have been analyzed with quasi-linear equations. The analysis has shown that the differential mobility appearing in the relaxation time of the large-signal analysis is not the same as that used in the small-signal analysis. The differential mobility of the large-signal analysis, however, becomes equal to that of the small-signal analysis when the domain reduces to a perturbation. It has been shown in the analysis that an equivalent admittance of a domain is represented by a parallel connection of capacitance and conductance which vary with time in the trnasient state. The time-constant of the admittance has been shown to equal the dielectric relaxation time plus a term dependent on the diffusion effect. The shape of a domain with a fractional depletion of carriers in the leading edge is expressed by a symmetrical triangle. The shape of a domain with a complete depletion, however,

is expressed by an asymmetrical triangle in which the gradient of the leading edge is determined by the density of the ionized impurity and the shape of the trailing edge is determined by the diffusion effect. The maximum value of the domain potential in a diode biased at the threshold has been derived to be approximately 54 % of the threshold voltage. The displacement current of the diode has been shown numerically to be very small in comparison with the conduction current. Thus the total current of the diode is given by the conduction current. The characteristics of a domain calculated from the results of the analysis have been given as numerical examples, which show qualitatively good agreement with the measured values of experiments. In further results derived from the study on the transient behavior of a high-field domain, it has been pointed out that non-linear and parametric operations can be interpreted by the use of an expression for admittance of the diode in whcih the effects of rf circuit voltage on the domain are taken into account.

(6) In the study on the magnetic field effects on the electron transfer and transport properties, it has been found theoretically and experimentally that the magnetic field decreases not only the drift velocity along the applied electric field but also the energy in the random motion of the electrons in a single valley; the former is known as the magnetoresistance effect and the latter can be termed the magnetic cooling effect. The cooling effect has been understood due to the decrease in the drift velocity of electrons in each valley and the appearently reduced value of the collision time

caused by the application of the magnetic field. The effects of the magnetic field on the velocity-field characteristic can be summarized as follows: (i) the drift velocity along the electric field decreases in a low-field region where the magnetoresistance effect predominates, whereas it increases (*i.e.*, a negative magnetoresistance effect) in a high-field region; (ii) the threshold field shifts to a higher field because the magnetic cooling effect requires higher intensity of field for the electron transfer to realize a negative differential mobility; (iii) the peak value of the total drift velocity increases, *i.e.*, a negative magnetoresistance effect, because more electrons are left in a lower valley with a high mobility; (iv) the differential mobility ($\partial v_{dy}/\partial E_x$) can be negative; and (v) the energy in the random motion and the diffusion coefficient decrease in a low-field region and increase in a high-field region. The experiment to measure the current-field characteristic by the microwave technique has shown qualitative agreements with the characteristic obtained by the theory. With this study, the qualitative understanding has been obtained to the electron transport properties of the transferred-electron semiconductors subjected to the crossed electric and magnetic fields. The results obtained can give the basis for the dynamic operations of the transferred-electron diodes subjected to the crossed fields.

(7) In a further study on the electronic properties of the transferred-electron semiconductors, new wave instabilities caused by a negative field dependency of the carrier temperature

have been derived. The diffusion instability, which is caused by a negative field dependency of the diffusion effect, has also been derived for an extrinsic semiconductor. It has been shown, however, that a negative value of the effective diffusion coefficient does not always lead to wave instability. The analysis is equally valid for a collision-dominated, weakly ionized gas, although it has been presented with reference to semiconductors.

Through the investigations in the condition for a differential negative resistance, the maximum available output power, self-pumped operation, transient behavior of a high-field domain, magnetic field effects, and wave instabilities by negative field dependency of the carrier temperature, the electronic and microwave properties of the transferred-electron semiconductors have been described in this thesis.

It can be suggested for further study that: (1) the noise figure in a self-pumped parametric operation of transferred-electron diodes; (2) the magnetic field effect taking account of the Hall field; (3) the experiment on a negative differential mobility subjected to the crossed electric and magnetic fields; and (4) materials for the wave instability due to a negatvie field dependency of the carrier temperature. These are in practical applications very interesting and important subjects which can be extended from the study in this thesis.

APPENDIX

The value of ω_i can be negative when $T_1 \gtrless 0$ and $(1+CT_1) \pm \{[(A^2+B^2)^{1/2}-A]/2\}^{1/2} \lesseqgtr 0$.

Case 1

$$T_1>0 \quad \text{and} \quad (1+CT_1)+\{[(A^2+B^2)^{1/2}-A]/2\}^{1/2}<0.$$

No condition occurs where both inequalities are satisfied simultaneously.

Case 2

$$T_1>0 \quad \text{and} \quad (1+CT_1)-\{[(A^2+B^2)^{1/2}-A]/2\}^{1/2}<0. \tag{A1}$$

Squaring inequality (A1), we obtain

$$2(1+CT_1)^2+A<(A^2+B^2)^{1/2}. \tag{A2}$$

Regardless of the values of A and B, we may have

$$-(A^2+B^2)^{1/2}<2(1+CT_1)^2+A. \tag{A3}$$

Thus, the square of the inequality (A2) gives $[2(1+CT_1)^2+A]^2<A^2+B^2$, which leads to $v_1T_1<0$. In case 2 the condition for ω_i to be negative is $v_1<0$ and $T_1>0$.

Case 3

$$T_1<0 \quad \text{and} \quad (1+CT_1)+\{[(A^2+B^2)^{1/2}-A]/2\}^{1/2}>0. \tag{A4}$$

In inequality (A4) we must consider two cares:

$$[(A^2+B^2)^{1/2}-A]^{1/2}>2^{1/2}(1+CT_1)>-[(A^2+B^2)^{1/2}-A]^{1/2}, \tag{A5}$$

$$2^{1/2}(1+CT_1)>[(A^2+B^2)^{1/2}-A]^{1/2}, \tag{A6}$$

where the second case is the same as case 4. We derive here the condition for the first case. Squaring inequality (A6) twice and considering inequality (A3), we obtain $v_1T_1<0$. The condition for ω_i to be negative is $v_1>0$ and $T_1<0$.

Case 4

$$T_1<0 \quad \text{and} \quad (1+CT_1)-\{[(A^2+B^2)^{1/2}-A]/2\}^{1/2}>0. \tag{A7}$$

The inequality (A7) requires that $(1+CT_1)$ is positive. Thus, T_1 is restricted to the range, $-1/C<T_1<0$.

Squaring inequality (A7), we have

$$2(1+CT_1)^2+A>(A^2+B^2)^{1/2} \tag{A8}$$

which requires that $[2(1+CT_1)^2+A]$ is positive. Provisionally assuming it to be positive and squaring inequality (A8), we obtain $v_1T_1>0$. Thus, in case 4 the condition for ω_i to be negative is $v_1<0$ and $-1/C<T_1<0$. The values v_1 and T_1 in the ranges obtained do not violate the assumption that $[2(1+CT_1)^2+A]$ is positive.

REFERENCES AND NOTES

Chapter II

[1] B. W. Hakki and S. Knight, "Microwave phenomena in bulk GaAs," *IEEE Trans. on Electron Devices*, vol. ED - 13, pp. 94 - 105, January 1966.

[2] J. B. Gunn, "Instabilities of current in III-V semiconductors," *IBM J. Res. and Dev.*, vol. 8, pp. 141 - 159, April 1964.

[3] H. Thim, M. Barber, B. W. Hakki, S. Knight, and M. Uenohara, "Microwave amplification in a dc-biased bulk semiconductor," *Appl. Phys. Letters*, vol. 7, pp. 167 - 168, September 1965.

[4] H. W. Thim and M. R. Barber, "Microwave amplification in a GaAs bulk semiconductor," *IEEE Trans. on Electron Devices*, vol. ED - 13, pp. 110 - 114, January 1966.

[5] D. E. McCumber and A. G. Chynoweth, "Theory of negative-conductance amplification and of Gunn instabilities in 'two-valley' semiconductors," *IEEE Trans. on Electron Devices*, vol. ED - 13, pp. 4 - 21, January 1966.

[6] By using the papers: R. W. H. Engelmann and C. F. Quate, "Linear, or 'small-signal,' theory for the Gunn effect," *IEEE Trans. on Electron Devices*, vol. ED - 13, pp. 44 - 52, January 1966; K. Blötekjaer and C. F. Quate, "The coupled modes of acoustic waves and drifting carriers in piezoelectric crystals," *Proc. IEEE*, vol. 52, pp. 360 - 377, April 1964; and footnote 5, we obtain the equivalent impedance (2.1).

[7] B. K. Ridley, "The inhibition of negative resisitance dipole waves and domains in n - GaAs," *IEEE Trans. on Electron Devices*, vol. ED - 13, pp. 41 - 43, January 1966. This paper derived the condition $n_0 L^2 > 10^9$ cm^{-1} from the inhibition of dipole waves and domains and from the assumption of the negative resistivity being taken to be larger than the ohmic resistivity by a factor of 10^2.

CHAPTER III

[1] D. E. McCumber and A. G. Chynoweth, "Theory of negative-conductance amplification and of Gunn instabilities in 'two-valley' semiconductors," *IEEE Trans. on Electron Devices*, vol. ED - 13, pp. 4 - 21, Jan-

uary 1966.

[2] A. Sasaki and T. Takagi, "Conditions for amplification, oscillation in GaAs bulk semiconductor," *Proc. IEEE*, vol. 54, pp. 2027 - 2028, December 1966.

[3] B. W. Hakki and S. Knight, "Microwave phenomena in bulk GaAs," *IEEE Trans. on Electron Devices*, vol. ED - 13, pp. 94 - 105, January 1966.

[4] H. Thim, M. Barber, B. W. Hakki, S. Knight, and M. Uenohara, "Microwave amplification in a dc-biased bulk semiconductor," *Appl. Phys. Letters*, vol. 7, pp. 167 - 168, September 1965.

[5] D. E. McCumber, private communication.

CHAPTER IV

[1] J. B. Gunn, "Instabilities of current in III - V semiconductors," *IBM J. Res. and Dev.*, vol. 8, pp. 141 - 159, April 1964.

[2] E. O. Johnson, "Physical limitations on frequency and power parameters of transistors," *RCA Rev.*, vol. 26, pp. 163 - 177, June 1965.

[3] P. N. Butcher and W. Fawcett, "Calculation of the velocity-field characteristics for gallium arsenide," *Phys. Lett.*, vol. 21, pp. 489 - 490, June 15, 1966.

CHAPTER V

[1] J. E. Caroll, "Mechanisms in Gunn effect microwave oscillators," *Radio Electron, Eng.*, vol. 34, pp. 17 - 30, July 1967.

[2] A. Sasaki, "Transient behaviour and characteristics of the high-field domain in Gunn-effect diodes," *Radio Electron. Eng.*, vol. 39, pp. 81 - 92, February 1970.

[3] J. E. Carroll, "Resonant-circuit operation of Gunn diode, a self-pumped parametric oscillator," *Electron. Lett.*, vol. 2, pp. 215 - 216, June 1966.

[4] C. S. Aitchsion, "Possible Gunn-effect parametric amplifier," *Electron. Lett.*, vol. 4, pp. 15 - 16, January 12, 1968.

[5] C. S. Aitchison, C. D. Corbey, and B. H. Newton, "Self-pumped Gunn-effect parametric amplifier," *Electron. Lett.*,vol. 5, pp. 36 - 37, January 23, 1969.

[6] A. Sasaki, "Admittance and its parametric effect of Gunn-effect diodes," presented at the Electron Devices Group Meeting, Inst. of Electron. and Elec. Commun. Engs. (IEECE) of Japan, March 1968, paper ED 67 - 53.

[7] A. Sasaki, "Parametric change in admittance of Gunn-effect diodes," presented at the Electron Devices Group Meeting, IEECE of Japan, October 1969, paper ED 69 - 29.

CHAPTER VI

[1] G. S. Hobson, "Small-signal admittance of a Gunn-effect device," *Electron. Lett.*, vol. 2, pp. 207 - 208, June 1966.

[2] D. E. McCumber and A. G. Chynoweth, "Theory of negative-conductance amplification and of Gunn instabilities in 'two-valley' semiconductor," *IEEE Trans. on Electron Devices*, vol. ED - 13, pp. 4 - 21, January 1966.

[3] A. Sasaki and T. Takagi, "Conditions for space-charge-wave growth and differential negative resistance in 'two-valley' semiconductor," *Proc. IEEE*, vol. 55, p. 732, May 1967.

[4] P. N. Butcher, W. Fawcett, and C. Hilsum, "A simple analysis of stable domain propagation in the Gunn effect," *Brit. J. Appl. Phys.*, vol. 17, pp. 841 - 850, July 1966.

[5] H. Kroemer, "Non-linear space-charge domain dynamics in a semiconductor with negative differential mobility," *IEEE Trans. on Electron Devices*, vol. ED - 13, pp. 27 - 40, January 1966.

[6] M. Shoji, "Bulk semiconductor high-speed current waveform generator," *Proc. IEEE*, vol. 55, pp. 720 - 721, May 1967.

[7] B. W. Hakki, "GaAs post threshold microwave amplifier, mixer, and oscillator," *Proc. IEEE*, vol. 54, pp. 299-300, February 1966.

[8] S. Sugimoto, "Up-conversion with Gunn-effect diode," *Proc. IEEE*, vol. 55, p. 1520, August 1967.

[9] J. E. Carroll, "Resonant-circuit operation of Gunn diode, a self-pumped parametric oscilltor," *Electron. Lett.*, vol. 2, pp. 215 - 216, June 1966.

[10] K. Kurokawa, "The dynamics of high-field propagating domains in bulk semiconductors," *Bell System Tech. J.*, vol. 46, pp. 2235 - 2259, December 1967.

[11] J. B. Gunn, "Instabilities of current in III - V semiconductors," *IBM J. Res. and Dev.*, vol. 8, pp. 141 - 159, April 1964.

[12] J. R. Haynes and W. Shockley, "Investigation of hole injection in transistor action," *Phys. Rev.*, vol. 75, p. 691, 15 February 1949.

[13] R. B. Adler, A. C. Smith, and R. L. Longini, *"Introduction to semiconductor physics,"* pp. 177 - 181 (Wiley, New York, 1964).

[14] J. B. Gunn, "On the shape of traveling domains in gallium arsenide," *IEEE Trans. on Electron Devices*, vol. ED - 14, pp. 720 - 721, October 1967.

[15] I. Kuru, P. N. Robson, and G. S. Kino, "Some measurements of the steady-state and transient characteristics of high-field dipole domain in GaAs," *IEEE Trans. on Electron Devices*, vol. ED - 15, pp. 21 - 29, January 1968.

[16] P. N. Butcher and W. Fawcett, "Calculation of the velocity-field characteristics for gallium arsenide," *Phys. Letters*, vol. 21, pp. 489 - 490, 15 June 1966.

[17] P. N. Butcher, W. Fawcett, and N. R. Ogg, "Effect of field dependent diffusion on stable domain propagation in the Gunn effect," *Brit. J. Appl. Phys.*, vol. 18, pp. 755 - 759, June 1967.

[18] R. B. Adler, *et al.*, *op. cit.*, p. 151.

[19] R. Harrison, "Simple transient and non-linear analysis of high-field domain in GaAs," *Brit. J. Appl. Phys. (J. Phys. D)*, Series 2, vol. 1, pp. 973 - 982, August 1968.

CHAPTER VII

[1] J. B. Gunn, "Instabilities of current in III - V semiconductors," *IBM J. Res. and Dev.*, vol. 8, pp. 141 - 159, April 1964.

[2] W. K. Kennedy, Jr., "Variation of the Gunn effect by magnetic field," *Proc. IEEE*, vol. 53, pp. 1639 - 1640, October 1965.

[3] K. Kekido, M. Takeuchi, Y. Takayama, F. Hasegawa, and Y. Hayakawa,

"Fabrication of planar-type GaAs bulk effect pulse devices," *Proc. the 1st. Conf. on Solid State Devices, J. Appl. Phys. supplement,* vol. 39, pp. 19 - 24, 1969, Tokyo.

[4] P. Guetin and C. Hervouet, "Decrease of the appearent threshold of the Gunn effect by transverse magnetic field," *Proc. IEEE,* vol. 56, pp. 1597 - 1598, September 1968.

[5] V. N. Vorobyev and V. S. Etkin, "Investigation of Gunn effect in a magnetic field," *Radio and Electro.,* vol. 14, pp. 358 - 361, 1969.

[6] G. A. Acket, "Microwave Hall mobility of hot electrons in gallium arsenide," *Philips Res. Rep.,* vol. 22, pp. 541 - 552, 1967.

[7] G. A. Acket, "Galvanomagnetic effects of hot electrons in gallium arsenide," *Philips Res. Rep.,* vol. 23, pp. 317 - 331, 1968.

[8] A. D. Boardman and W. Fawcett, "Effect of a magnetic field on inter-band electron transfer in gallium arsenide," *Phys. Letters,* vol. 29A p. 430, 30 June 1969.

[9] H. C. Law and K. C. Kao, "High-field galvanomagnetic effects in two-valley n-type semiconductors," *Solid-State Electro.,* vol. 13, pp. 1223 - 1230, September 1970.

[10] E. M. Conwell and M. O. Vassel, "High-field transport in n-type GaAs," *Phys. Rev.,* vol. 166, pp. 797 - 821, 15 February 1968.

[11] J. Yamashita and M. Watanabe, "On the conductivity of non-polar crystals in the strong electric field, I," *Progr. theor. Phys.,* vol. 12, pp. 443 - 453, October 1954.

[12] A. Sasaki, H. Oheda, and T. Tanaka, "Effects of magnetic field on electron transfer and velocity-field characteristic in gallium arsenide," *J. phys. Soc. Japan,* vol. 32, pp. 1550 - 1555, June 1972.

[13] N. Hashizume and S. Kataoka," Carrier wave in n type gallium arsenide under crossed d.c. electric and magnetic fields," *Proc. IEE,* vol. 119, pp. 505 - 511, May 1972.

[14] P. N. Butcher and W. Fawcett, "The intervalley transfer mechanism of negative resistivity in bulk semiconductors," *Proc. Phys. Soc.,* vol. 86, pp. 1205 - 1219, 1965.

[15] W. Fawcett, A. D. Boardman,and S. Swain, "Monte Carlo determination

of electron transport properties in gallium arsenide," *J. Phys. Chem. Solids*, vol. 31, pp. 1963 - 1990, September 1970.

[16] W. Heinle, "Displaced Maxwellian calculation of transport in n-type GaAs," *Phys. Rev.*, vol. 178, pp. 1319 - 1325, 15 February 1969.

[17] N. Braslau and P. S. Hauge, "Microwave measurement of the velocity-field characteristic of GaAs at microwave frequencies," *IEEE Trans. on Electron Devices*, vol. ED - 17, pp. 616 - 622, August 1970.

[18] J. Zuker, V. J. Fowler, and E. M. Conwell, "High-field conductivity in germanium and silicon at microwave frequencies," *J. Appl. Phys.*, vol. 32, pp. 2606 - 2610, December 1961.

[19] J. B. Gunn, *J. Electro.* vol. 2, p. 87, 1956.

CHAPTER VIII

[1] T. Misawa, "Negative resistance in p - n junctions under avalanche breakdown conditions, Part I," *IEEE Trans. on Electron Devices*, vol. ED - 13, pp. 137 - 143, January 1966.

[2] D. E. McCumber and A. G. Chynoweth, "Theory of negative-conductance amplification and of Gunn instabilities in 'two-valley' semiconductor," *IEEE Trans. on Electron Devices*, vol. ED - 13, pp. 4 - 21, January 1966.

[3] K. Blotakjaer and P. Weissglas, "Diffusion instabilities in semiconductors," *Phys. Rev.*, vol. 39, pp. 1645 - 1653, 15 February 1968, and D. W. Ross, "Oscillations of a weakly ionized plasma in a strong electric field," *Phys. Rev.*, vol. 146, pp. 178 - 186, 3 June 1966.

[4] K. Blotekjaer, *Ericsson Tech.*, vol. 22, p. 125, 1966.

[5] E. H. Holt and R. E. Haskell, "*Foundations of plasma dynamics*," 1st ed., p. 151 (Macmillan, New York, 1965).

[6] When $T_0 \gg T_{L0}$ can be assumed, we may obtain the value of the energy relaxation time $\tau_{e0} = 3k\mu_0 T_0/qv_0^2$ by measuring the diffusion coefficient $k\mu_0 T_0/q$ and the drift velocity v_0.

[7] R. J. Briggs, "*Electron-stream interaction with plasmas*," p. 8 (MIT Press, Cambridge, Mass., 1964).

[8] J. E. Carroll, "Nonisothermal waves on charge carrier streams," *IEEE*

Trans. on Electron Devices, vol. ED - 13, pp. 187 - 189, January 1966.

[9] It must be noted that the existence of an unstable wave does not always produce negative conductance in a semiconductor because of simultaneous existence of attenuated wave.

ADDENDUM

The contents of the thesis consist of eight papers published in scientific and technical journals in Japan and foreign countries. Those are

(1) "Conditions for amplification, oscillation in GaAs bulk semiconducotr," by A. Sasaki and T. Takagi, Proc. IEEE (U. A. S.), vol. 54, pp. 2027 - 2028, December 1966, which is written in Chapter II,

(2) "Conditions for space-charge-wave growth and differential negative resistance in 'two-valley' semiconductors," by A. Sasaki and T. Takagi, Proc. IEEE (U. S. A.), vol. 55, p. 732, May 1967, which is written in Chapter III,

(3) "Frequency dependencies of power and efficiency of transit-time oscillations in two-valley semiconductors," by A. Sasaki, Proc. IEEE (U. S. A.), vol. 56, p. 1757, October 1968, which is written in Chapter IV,

(4) "Self-pumped parametric amplification and oscillation of Gunn-effect diodes," by A. Sasaki, Proc. IEEE (U. S. A.), vol. 59, pp. 89 - 90, January 1971, which is written in Chapter V,

(5) "Transient behaviour and characteristics of the high-field domain in Gunn-effect diodes," by A. Sasaki, Radio and Electronic Engineer (Great Britain), vol. 39, pp. 81 - 92, February 1970, which is written Chapter VI,

(6) "Effects of magnetic field on electron transport properties in gallium arsenide," by A. Sasaki and T. Tanaka, Proc. 3rd Conf. Solid State Devices, Tokyo, 1971, Supplement to OYO

BUTURI (Japan), vol. 41, pp. 24 - 29, which is written in Chapter VII,

(7) "Effects of magnetic field on electron transfer and velocity-field characteristic in gallium arsenide," by A. Sasaki, H. Oheda, and T. Tanaka, J. Phys. Soci. Japan (Japan), vol. 32, pp. 1550 - 1555, June 1972, some of which is written in Chapter VII, and

(8) "Wave instabilities in bulk semiconductors with field-dependent drift velocity and carrier temperature," by A. Sasaki, J, Appl. Phys. (U. S. A.), vol. 41, pp. 3813 - 3818, August 1970, which is written in Chapter VIII.

Through these papers, the thesis describes electronic and microwave properties of transferred-electron semiconductors.